This article has been accepted for publication in a future issue of this journal, but has not been fully edited. Content may change prior to final publication. Citation information: DOI 10.1109/TWC.2016.2630680, IEEE Transactions on Wireless Communications

Dual-Hop FSO Transmission Systems over Gamma-Gamma Turbulence with Pointing Errors

Emna Zedini, *Student Member, IEEE,* Hamza Soury, *Student Member, IEEE,* and Mohamed-Slim Alouini, *Fellow, IEEE*

***Abstract*—In this paper, we analyze the end-to-end performance of dual-hop free-space optical (FSO) fixed gain relaying systems under heterodyne detection and intensity modulation with direct detection techniques in the presence of atmospheric turbulence as well as pointing errors. In particular, we derive the cumulative distribution function (CDF) of the end-to-end signal-to-noise ratio (SNR) in exact closed-form in terms of the bivariate Fox's H function. Capitalizing on this CDF expression, novel closed-form expressions for the outage probability, the average bit-error rate (BER) for different modulation schemes, and the ergodic capacity of dual-hop FSO transmission systems are presented. Moreover, we present very tight asymptotic results for the outage probability and the average BER at high SNR regime in terms of simple elementary functions and we derive the diversity order of the considered system. By using dual-hop FSO relaying, we demonstrate a better system performance as compared to the single FSO link. Numerical and Monte-Carlo simulation results are provided to verify the accuracy of the newly proposed results, and a perfect agreement is observed.**

***Index Terms*—Free-space optics (FSO), dual-hop relaying, pointing errors, Gamma-Gamma, outage probability, average bit-error rate (BER), ergodic capacity.**

I. Introduction

Free-space optical (FSO) communication systems have gained a growing research interest due to their various features. These include high data rates due to their very high bandwidth, with high security level at the unlicensed optical spectrum, robustness to electromagnetic interference, and ease of deployment among others. This promising technology is able to overcome the spectrum scarcity issue in wireless communications systems [1]–[8].

However, fluctuations in both the phase and the intensity of the received signal caused by the atmospheric turbulence may lead to a severe performance degradation, especially over a range of several kilometers [1]. Several statistical channel models have been presented to characterize the turbulence-induced fading in FSO systems, and Gamma-Gamma distribution is the most suitable model to characterize moderate to strong turbulence regimes [9]. Moreover, FSO transmission is sensitive to weather conditions, such as rain, aerosols, and particularly fog. This dependence on the atmospheric conditions can significantly affect the reliability of FSO systems. Furthermore, thermal expansion, wind loads, and small earthquakes cause building sway that results in deviation of the beam from its original path. This misalignment between the transmitter and the receiver, known as pointing error, can significantly impact the quality of FSO links [10].

FSO systems can be classified into two categories based on the detection type at the receiver side, namely coherent and non-coherent. Non-coherent systems, also known as intensity modulation with direct-detection (IM/DD), are commonly used in FSO links mainly because of their simplicity and low cost [6]. In such systems, the receiver directly detects the intensity of the emitted light. With recent advances in integrated circuits as well as high-speed digital signal processing, coherent detection is becoming more attractive [11]–[14]. In such systems, the incoming optical signal is mixed with a local oscillator (LO) before photo-detection, which improves the receiver sensitivity [15], [16]. Another interesting property of coherent detection is that amplitude, frequency, and phase modulation can be employed, which considerably increase the system spectral efficiency [14]. Furthermore, coherent detection allows background noise rejection [17]. Coherent systems can be further categorized into two classes, homodyne and heterodyne systems. In homodyne detection, the LO is running at the same frequency as the incoming radiation while in heterodyne detection, the frequency of the local oscillator and the incoming radiation can be different.

Relaying technique has been demonstrated as an efficient solution to mitigate the short range as well as the turbulence-induced fading. By using short hops, this technology can broaden the coverage and improve the FSO link performance [18]–[21]. As such, considerable efforts have been devoted to study the relay system performance when FSO and radio-frequency (RF) are used in series in the so-called mixed RF/FSO systems under both heterodyne and IM/DD techniques employing decode-and-forward (DC) or amplify-and-forward (AF) relaying [22]–[30]. In such system models, multiple RF users can be multiplexed and sent over the FSO link. This also has increased the interest to study the performance of dual-hop mixed FSO/RF systems, where the FSO link is used as a broadcast channel that serves different RF users. As per authors' best knowledge, the first exact closed-form performance analysis of dual-hop FSO/RF fixed gain relaying systems has been carried out in [31]. Having such interesting results motivates further the analysis of dual-

This work was supported in part by the Qatar National Research Fund (a member of Qatar Foundation) under NPRP Grant NPRP9-077-2-036. The statements made herein are solely the responsibility of the authors.

E. Zedini and M.-S. Alouini are with the Computer, Electrical, and Mathematical Science and Engineering (CEMSE) Division, King Abdullah University of Science and Technology (KAUST) Thuwal, Makkah Province, Saudi Arabia (e-mail:{emna.zedini,slim.alouini}@kaust.edu.sa).

This work was done when H. Soury was a PhD student with the CEMSE division at KAUST. He is now with the Electrical and Computer Engineering, University of Illinois at Chicago (UIC), USA (e-mail: soury.hamza@kaust.edu.sa).

This article has been accepted for publication in a future issue of this journal, but has not been fully edited. Content may change prior to final publication. Citation information: DOI 10.1109/TWC.2016.2630680, IEEE Transactions on Wireless Communications

hop FSO fixed gain relaying communication systems. In [32], bounds for the performance analysis of dual-hop FSO system with channel-state information (CSI)-assisted amplify-and-forward (AF) relay are presented. An experimental setup of an all-optical 10-Gbps dual-hop FSO system using an AF relay has been presented in [33].

Highly motivated by the experimental verification in [33], this paper studies the end-to-end performance of dual-hop FSO systems in exact closed-form. To the best of the authors' knowledge, this represents the first exact closed-form performance study of such systems. Indeed, the use of fixed gain relay introduces a shift in the expression of the end-to-end signal-to-noise ratio (SNR) making the analysis quite challenging. Hence, we develop a new analytical framework to evaluate the performance of dual-hop FSO systems with either of the two types of detection techniques (i.e. IM/DD or heterodyne detection) under the combined effect of atmospheric turbulence and pointing errors. The results show a significant improvement in the performance of the dual-hop FSO system over the single FSO link and are as such in a perfect agreement with what was observed experimentally in [33]. More specifically, we derive the cumulative distribution function (CDF) of such systems in terms of the bivariate Fox's H function. Then, we derive the performance metrics such us the outage probability, the average bit-error rate (BER) for different modulation schemes, and the ergodic capacity of the dual-hop FSO system. At high SNR, we provide very tight asymptotic results for the outage probability and the average BER in terms of simple elementary functions, and we derive the diversity order of the considered system.

The remainder of this paper is organized as follows. In Section II, we introduce the channel and communication system model. We derive the cumulative distribution function (CDF), the probability density function (PDF), the moment generating function (MGF), and the moments of the end-to-end signal-to-noise ratio (SNR) of dual-hop FSO systems in Section III. Capitalizing on these results, we present closed-form expressions of the outage probability, the average BER, and the ergodic capacity along with the asymptotic analysis at high SNR regime in Section IV. Section V presents some numerical and simulation results to illustrate the mathematical formalism presented in the previous section. Finally, some concluding remarks are drawn in Section VI.

II. Channel and System Models

We consider a dual-hop optical communication system where the source terminal S is communicating with the destination terminal D through a half-duplex relay terminal R. The two FSO hops (i.e. S-R and R-D) are assumed to be subject to independent but not necessarily identically distributed Gamma-Gamma fading that accounts for pointing errors and both types of detection techniques (i.e. IM/DD as well as heterodyne detection). In this paper, we assume a high-energy FSO system whose performance is limited by shot noise as well as thermal noise. In this case, the noise can be modeled to high accuracy as zero mean, signal independent additive white Gaussian noise (AWGN) (a widely accepted assumption in many reported works in the literature [34]–[37]).

The overall instantaneous SNR of a dual-hop FSO system employing AF equipped with fixed gain relay under the assumption of negligible saturation can be written as [38] [1]

$$\gamma = \frac{\gamma_1 \gamma_2}{\gamma_2 + C}, \tag{1}$$

where C is a constant inversely proportional to the squared relay's gain [38], and γ_i is the instantaneous SNR of the ith hop for $i \in (1, 2)$ with the PDF given in [29, Eq.(3)] as

$$f_{\gamma_i}(\gamma_i) = \frac{\xi_i^2}{r_i\, \Gamma(\alpha_i)\, \Gamma(\beta_i)\, \gamma_i} \times \mathrm{G}_{1,3}^{3,0}\left[\alpha_i\, \beta_i\, h_i \left(\frac{\gamma_i}{\mu_{r_i}}\right)^{\frac{1}{r_i}} \middle| \begin{matrix} \xi_i^2 + 1 \\ \xi_i^2, \alpha_i, \beta_i \end{matrix}\right], \tag{2}$$

where $h_i = \frac{\xi_i^2}{\xi_i^2+1}$, r_i is the parameter that represents the type of detection being used (i.e. $r_i = 1$ is associated with heterodyne detection and $r_i = 2$ associated with IM/DD), ξ_i denotes the ratio between the equivalent beam radius at the receiver and the pointing error displacement standard deviation (jitter) at the receiver given as $\xi_i = \frac{w_{z_{eq},i}}{2\,\sigma_{s,i}}$, with $\sigma_{s,i}^2$ is the jitter variance at the receiver and $w_{z_{eq},i}$ is the equivalent beam radius at the receiver [10], $\mathrm{G}_{\cdot,\cdot}^{\cdot,\cdot}(\cdot)$ is the Meijer's G function, and μ_{r_i} refers to the average electrical SNR of the ith hop. In particular, for $r_i = 1$,

$$\mu_{1_i} = \mu_{\mathrm{heterodyne}_i} = \mathbb{E}[\gamma_i] = \overline{\gamma}_i, \tag{3}$$

and for $r_i = 2$,

$$\mu_{2_i} = \mu_{\mathrm{IM/DD}_i} = \frac{\alpha_i\, \beta_i\, \xi_i^2\, (\xi_i^2 + 2)}{(\alpha_i + 1)(\beta_i + 1)(\xi_i^2 + 1)^2}\overline{\gamma}_i, \tag{4}$$

with α_i and β_i the fading parameters related to the atmospheric turbulence conditions [3]. More specifically, assuming a plane wave propagation in the absence of inner scale, α_i and β_i can be determined from the Rytov variance as [3]

$$\alpha_i = \left[\exp\left(\frac{0.49\,\sigma_{R,i}^2}{\left(1 + 1.11\,\sigma_{R,i}^{12/5}\right)^{7/6}}\right) - 1\right]^{-1} \tag{5}$$

$$\beta_i = \left[\exp\left(\frac{0.51\,\sigma_{R,i}^2}{\left(1 + 0.69\,\sigma_{R,i}^{12/5}\right)^{5/6}}\right) - 1\right]^{-1}, \tag{6}$$

where $\sigma_{R,i}^2 = 1.23\, C_{n,i}^2 \left(\frac{2\pi}{\lambda_i}\right)^{\frac{7}{6}} L_i^{\frac{11}{6}}$ is the Rytov variance, $C_{n,i}^2$ denotes the refractive-index structure parameter, λ_i is the wavelength, and L_i represents the propagation distance of the ith hop for $i \in (1, 2)$. Moreover, by using [39, Eq.(2.24.2/3)] then [40, Eq.(2.4.5)], we can obtain the CDF of γ_i as

$$F_{\gamma_i}(\gamma_i) = 1 - \frac{\xi_i^2}{\Gamma(\alpha_i)\, \Gamma(\beta_i)} \times \mathrm{G}_{2,4}^{4,0}\left[\alpha_i\, \beta_i\, h_i \left(\frac{\gamma_i}{\mu_{r_i}}\right)^{\frac{1}{r_i}} \middle| \begin{matrix} 1, \xi_i^2 + 1 \\ 0, \xi_i^2, \alpha_i, \beta_i \end{matrix}\right]. \tag{7}$$

[1] For tractability, we neglect the saturation effect of the relay amplifier.

This article has been accepted for publication in a future issue of this journal, but has not been fully edited. Content may change prior to final publication. Citation information: DOI 10.1109/TWC.2016.2630680, IEEE Transactions on Wireless Communications

III. End-to-End SNR Statistics

A. Cumulative Distribution Function

1) Exact Analysis: The CDF of the overall SNR, γ, for a dual-hop FSO system under both types of detection techniques (i.e. heterodyne detection as well as IM/DD) with pointing errors taken into account can be given in exact closed form as

$$F_{\gamma}(\gamma) = 1 - \frac{\xi_1^2\,\xi_2^2}{r_1\,r_2\,\Gamma(\alpha_1)\Gamma(\alpha_2)\Gamma(\beta_1)\Gamma(\beta_2)}\mathrm{H}_{1,0:1,4:3,2}^{0,1:4,0:0,3}\left[\begin{array}{c|c} (1,\frac{1}{r_2},\frac{1}{r_1}) & \\ - & \\ (1+\xi_2^2,1) & \\ (\xi_2^2,1),(\alpha_2,1),(\beta_2,1),(0,\frac{1}{r_2}) & \alpha_2\beta_2 h_2\left(\frac{C}{\mu_{r_2}}\right)^{\frac{1}{r_2}}, \frac{\left(\frac{\mu_{r_1}}{\gamma}\right)^{\frac{1}{r_1}}}{\alpha_1\beta_1 h_1} \\ (1-\xi_1^2,1)(1-\alpha_1,1)(1-\beta_1,1) & \\ (-\xi_1^2,1)(0,\frac{1}{r_1}) & \end{array}\right], \tag{8}$$

where $\mathrm{H}_{\cdot,\cdot:\cdot,\cdot:\cdot,\cdot}^{\cdot,\cdot:\cdot,\cdot:\cdot,\cdot}(\cdot,\cdot)$ is the bivariate Fox's H function, known also as the Fox's H function of two variables [41] whose MATLAB implementation is presented in [42].

Proof: See Appendix A. ∎

It is worthy to mention that for the special case where the two FSO hops operate under heterodyne detection, i.e. $r_1 = 1$ and $r_2 = 1$, the unified expression given by (8) can be simplified in terms of the extended generalized bivariate Meijer's G function, $\mathrm{G}_{\cdot,\cdot:\cdot,\cdot:\cdot,\cdot}^{\cdot,\cdot:\cdot,\cdot:\cdot,\cdot}$ with the help of [40, Eq.(2.9.1)] as

$$F_{\gamma}^{H}(\gamma) = 1 - \frac{\xi_1^2\,\xi_2^2}{\Gamma(\alpha_1)\Gamma(\alpha_2)\Gamma(\beta_1)\Gamma(\beta_2)}\mathrm{G}_{1,0:1,4:3,2}^{0,1:4,0:0,3}\left[\begin{array}{c|c} 1 & \\ - & \\ \xi_2^2,\alpha_2,\beta_2,0 & \begin{array}{c} 1+\xi_2^2 \\ -\end{array} \end{array}\right. \left.\begin{array}{c} 1-\xi_1^2,1-\alpha_1,1-\beta_1 \\ -\xi_1^2,0 \end{array}\right| \frac{\alpha_2\beta_2 h_2 C}{\mu_{r_2}}, \frac{\mu_{r_1}}{\alpha_1\beta_1 h_1\gamma}\Bigg]. \tag{9}$$

Note that an efficient MATHEMATICA implementation for $\mathrm{G}_{\cdot,\cdot:\cdot,\cdot:\cdot,\cdot}^{\cdot,\cdot:\cdot,\cdot:\cdot,\cdot}(\cdot,\cdot)$ is presented in [43, Table II].

2) High SNR Analysis: The exact expression of the CDF in (8) is derived in terms of the bivariate Fox's H function which is a quite complex function and is not a standard built-in function in most of the well-known mathematical software packages such as MATLAB and MATHEMATICA, and as such it reveals limited physical insights. Therefore, we present an asymptotic analysis of the CDF in the high SNR regime. In particular, a very tight asymptotic result for the CDF in (8) can be obtained by using [41, Eq.(1.1)] and [40, Eq.(1.8.4)] with some algebraic manipulations as shown by (10). It should be noted here that the CDF expression given in (10) includes only summations of basic elementary functions, as compared to the exact CDF expression derived in terms of the bivariate Fox's H function in (8). This result, being much more analytically tractable, is very accurate and converges perfectly to the exact result at high SNR. Interestingly enough, with the help of this simple result, one may easily derive the diversity order of the dual-hop FSO system in the presence of pointing errors for both heterodyne and IM/DD detection techniques. As can be seen from (10), the diversity order of the considered system is a function of the type of receiver detection being used in each hop (i.e. r_1 and r_2), the two FSO hop's turbulence parameters (i.e. α_1, β_1, α_2, and β_2), and the pointing errors (i.e. ξ_1 and ξ_2).

Proof: See Appendix B. ∎

It is important to note that this expression is very useful to obtain asymptotic results for the MGF and the average BER at high SNR range as will be shown in the next sections.

$$\begin{aligned}
F_{\gamma}(\gamma)_{\mu_{r_1},\mu_{r_2}\gg 1} \approx\; & \frac{\Gamma(\alpha_1-\xi_1^2)\Gamma(\beta_1-\xi_1^2)}{\Gamma(\alpha_1)\Gamma(\beta_1)}\left((\alpha_1\beta_1 h_1)^{r_1}\frac{\gamma}{\mu_{r_1}}\right)^{\frac{\xi_1^2}{r_1}} \\
& + \frac{\xi_1^2\Gamma(\beta_1-\alpha_1)}{(\xi_1^2-\alpha_1)\Gamma(1+\alpha_1)\Gamma(\beta_1)}\left((\alpha_1\beta_1 h_1)^{r_1}\frac{\gamma}{\mu_{r_1}}\right)^{\frac{\alpha_1}{r_1}} + \frac{\xi_1^2\Gamma(\alpha_1-\beta_1)}{(\xi_1^2-\beta_1)\Gamma(\alpha_1)\Gamma(1+\beta_1)}\left((\alpha_1\beta_1 h_1)^{r_1}\frac{\gamma}{\mu_{r_1}}\right)^{\frac{\beta_1}{r_1}} \\
& + \frac{\xi_2^2\Gamma(\alpha_1-\xi_1^2)\Gamma(\beta_1-\xi_1^2)\Gamma(\alpha_2-\xi_1^2\frac{r_2}{r_1})\Gamma(\beta_2-\xi_1^2\frac{r_2}{r_1})}{2(\xi_2^2-\xi_1^2\frac{r_2}{r_1})\Gamma(\alpha_1)\Gamma(\alpha_2)\Gamma(\beta_1)\Gamma(\beta_2)}\left((\alpha_1\beta_1 h_1)^{r_1}(\alpha_2\beta_2 h_2)^{r_2}\frac{C\gamma}{\mu_{r_1}\mu_{r_2}}\right)^{\frac{\xi_1^2}{r_1}} \\
& + \frac{\xi_1^2\xi_2^2\Gamma(\beta_1-\alpha_1)\Gamma(\alpha_2-\alpha_1\frac{r_2}{r_1})\Gamma(\beta_2-\alpha_1\frac{r_2}{r_1})}{2(\xi_1^2-\alpha_1)(\xi_2^2-\alpha_1\frac{r_2}{r_1})\Gamma(1+\alpha_1)\Gamma(\alpha_2)\Gamma(\beta_1)\Gamma(\beta_2)}\left((\alpha_1\beta_1 h_1)^{r_1}(\alpha_2\beta_2 h_2)^{r_2}\frac{C\gamma}{\mu_{r_1}\mu_{r_2}}\right)^{\frac{\alpha_1}{r_1}} \\
& + \frac{\xi_1^2\xi_2^2\Gamma(\alpha_1-\beta_1)\Gamma(\alpha_2-\beta_1\frac{r_2}{r_1})\Gamma(\beta_2-\beta_1\frac{r_2}{r_1})}{2(\xi_1^2-\beta_1)(\xi_2^2-\beta_1\frac{r_2}{r_1})\Gamma(\alpha_1)\Gamma(\alpha_2)\Gamma(1+\beta_1)\Gamma(\beta_2)}\left((\alpha_1\beta_1 h_1)^{r_1}(\alpha_2\beta_2 h_2)^{r_2}\frac{C\gamma}{\mu_{r_1}\mu_{r_2}}\right)^{\frac{\beta_1}{r_1}} \\
& + \frac{\xi_1^2\Gamma(\alpha_1-\xi_2^2\frac{r_1}{r_2})\Gamma(\beta_1-\xi_2^2\frac{r_1}{r_2})\Gamma(\alpha_2-\xi_2^2)\Gamma(\beta_2-\xi_2^2)}{(\xi_1^2-\xi_2^2\frac{r_1}{r_2})\Gamma(\alpha_1)\Gamma(\alpha_2)\Gamma(\beta_1)\Gamma(\beta_2)}\left((\alpha_1\beta_1 h_1)^{r_1}(\alpha_2\beta_2 h_2)^{r_2}\frac{C\gamma}{\mu_{r_1}\mu_{r_2}}\right)^{\frac{\xi_2^2}{r_2}} \\
& + \frac{\xi_1^2\xi_2^2\Gamma(\alpha_1-\alpha_2\frac{r_1}{r_2})\Gamma(\beta_1-\alpha_2\frac{r_1}{r_2})\Gamma(\beta_2-\alpha_2)}{(\xi_1^2-\alpha_2\frac{r_1}{r_2})(\xi_2^2-\alpha_2)\Gamma(\alpha_1)\Gamma(1+\alpha_2)\Gamma(\beta_1)\Gamma(\beta_2)}\left((\alpha_1\beta_1 h_1)^{r_1}(\alpha_2\beta_2 h_2)^{r_2}\frac{C\gamma}{\mu_{r_1}\mu_{r_2}}\right)^{\frac{\alpha_2}{r_2}} \\
& + \frac{\xi_1^2\xi_2^2\Gamma(\alpha_1-\beta_2\frac{r_1}{r_2})\Gamma(\beta_1-\beta_2\frac{r_1}{r_2})\Gamma(\alpha_2-\beta_2)}{(\xi_1^2-\beta_2\frac{r_1}{r_2})(\xi_2^2-\beta_2)\Gamma(\alpha_1)\Gamma(\alpha_2)\Gamma(\beta_1)\Gamma(1+\beta_2)}\left((\alpha_1\beta_1 h_1)^{r_1}(\alpha_2\beta_2 h_2)^{r_2}\frac{C\gamma}{\mu_{r_1}\mu_{r_2}}\right)^{\frac{\beta_2}{r_2}}.
\end{aligned} \tag{10}$$

This article has been accepted for publication in a future issue of this journal, but has not been fully edited. Content may change prior to final publication. Citation information: DOI 10.1109/TWC.2016.2630680, IEEE Transactions on Wireless Communications

B. Probability Density Function

Differentiating (8) with respect to γ results in the exact closed-form expression of the PDF of γ in terms of the bivariate Fox's H function, that is,

$$f_\gamma(\gamma) = \frac{\xi_1^2\,\xi_2^2}{r_1\,r_2\,\Gamma(\alpha_1)\Gamma(\alpha_2)\Gamma(\beta_1)\Gamma(\beta_2)\,\gamma}\mathrm{H}_{1,0:1,4:3,2}^{0,1:4,0:0,3}\left[\begin{matrix}(1,\frac{1}{r_2},\frac{1}{r_1})\\ -\\ (1+\xi_2^2,1)\\ (\xi_2^2,1),(\alpha_2,1),(\beta_2,1),(0,\frac{1}{r_2})\\ (1-\xi_1^2,1)(1-\alpha_1,1)(1-\beta_1,1)\\ (-\xi_1^2,1)(1,\frac{1}{r_1})\end{matrix}\middle|\begin{matrix}\\ \\ \\ \\ \\ \\ \end{matrix}\alpha_2\beta_2 h_2\left(\frac{C}{\mu_{r_2}}\right)^{\frac{1}{r_2}},\frac{\left(\frac{\mu_{r_1}}{\gamma}\right)^{\frac{1}{r_1}}}{\alpha_1\beta_1 h_1}\right]. \tag{11}$$

Proof: See Appendix C. ■

C. Moment Generating Function

1) Exact Analysis: The MGF, defined as $\mathcal{M}_\gamma(s) = \mathbb{E}[e^{-\gamma s}]$, can be expressed in terms of the CDF by using integration by parts as [23]

$$\mathcal{M}_\gamma(s) = s\int_0^\infty e^{-\gamma s}F_\gamma(\gamma)\,d\gamma. \tag{12}$$

Substituting the CDF expression derived in Appendix A into (12), and applying [44, Eq.(3.381/4)] then [41, Eq.(1.1)], the MGF of γ can be given in terms of the bivariate Fox's H function by

$$\mathcal{M}_\gamma(s) = 1 - \frac{\xi_1^2\,\xi_2^2}{r_1\,r_2\,\Gamma(\alpha_1)\Gamma(\alpha_2)\Gamma(\beta_1)\Gamma(\beta_2)}\mathrm{H}_{1,0:1,4:3,3}^{0,1:4,0:1,3}\left[\begin{matrix}(1,\frac{1}{r_2},\frac{1}{r_1})\\ -\\ (1+\xi_2^2,1)\\ (\xi_2^2,1),(\alpha_2,1),(\beta_2,1),(0,\frac{1}{r_2})\\ (1-\xi_1^2,1)(1-\alpha_1,1)(1-\beta_1,1)\\ (1,\frac{1}{r_1})(-\xi_1^2,1)(0,\frac{1}{r_1})\end{matrix}\middle|\begin{matrix}\\ \\ \\ \\ \\ \\ \end{matrix}\alpha_2\beta_2 h_2\left(\frac{C}{\mu_{r_2}}\right)^{\frac{1}{r_2}},\frac{(s\mu_{r_1})^{\frac{1}{r_1}}}{\alpha_1\beta_1 h_1}\right], \tag{13}$$

When $r_1 = 1$ and $r_2 = 2$, (13) becomes the MGF of dual-hop FSO systems using the heterodyne detection technique and can be represented in terms of the bivariate Meijer's G function as

$$\mathcal{M}_\gamma^H(s) = 1 - \frac{\xi_1^2\,\xi_2^2}{r_1\,r_2\,\Gamma(\alpha_1)\Gamma(\alpha_2)\Gamma(\beta_1)\Gamma(\beta_2)}\mathrm{G}_{1,0:1,4:3,3}^{0,1:4,0:1,3}\left[\begin{matrix}1\\ -\end{matrix}\middle|\begin{matrix}1+\xi_2^2\\ \xi_2^2,\alpha_2,\beta_2,0\end{matrix}\middle|\begin{matrix}1-\xi_1^2,1-\alpha_1,1-\beta_1\\ 1,-\xi_1^2,0\end{matrix}\middle|\begin{matrix}\frac{\alpha_2\beta_2 h_2 C}{\mu_{r_2}},\frac{s\,\mu_{r_1}}{\alpha_1\beta_1 h_1\gamma}\end{matrix}\right]. \tag{14}$$

2) High SNR Analysis: By substituting (10) into (12) then applying the integral identity [44, Eq.(3.381/4)], the MGF in (13) can be asymptotically expressed at high SNR in terms of basic elementary functions as shown by (15).

It is important to note here that the asymptotic result for the MGF in (15) is easily tractable and particularly useful to evaluate the average symbol error rate (SER) of M-PSK and M-QAM by applying the MGF-based approach. By utilizing this method, the SER can be calculated based entirely on knowledge of the MGF of the end-to-end SNR without ever having to compute its PDF and CDF [45].

$$\begin{aligned}
\mathcal{M}_\gamma(s)_{\mu_{r_1},\mu_{r_2}\gg 1} \approx\;& \frac{\Gamma(\alpha_1-\xi_1^2)\Gamma(\beta_1-\xi_1^2)\Gamma\left(1+\frac{\xi_1^2}{r_1}\right)}{\Gamma(\alpha_1)\Gamma(\beta_1)}\left(\frac{(\alpha_1\beta_1 h_1)^{r_1}}{s\mu_{r_1}}\right)^{\frac{\xi_1^2}{r_1}}\\
&+\frac{\xi_1^2\Gamma(\beta_1-\alpha_1)\Gamma\left(1+\frac{\alpha_1}{r_1}\right)}{(\xi_1^2-\alpha_1)\Gamma(1+\alpha_1)\Gamma(\beta_1)}\left(\frac{(\alpha_1\beta_1 h_1)^{r_1}}{s\mu_{r_1}}\right)^{\frac{\alpha_1}{r_1}}+\frac{\xi_1^2\Gamma(\alpha_1-\beta_1)\Gamma\left(1+\frac{\beta_1}{r_1}\right)}{(\xi_1^2-\beta_1)\Gamma(\alpha_1)\Gamma(1+\beta_1)}\left(\frac{(\alpha_1\beta_1 h_1)^{r_1}}{s\mu_{r_1}}\right)^{\frac{\beta_1}{r_1}}\\
&+\frac{\xi_2^2\Gamma(\alpha_1-\xi_1^2)\Gamma(\beta_1-\xi_1^2)\Gamma(\alpha_2-\xi_1^2\frac{r_2}{r_1})\Gamma(\beta_2-\xi_1^2\frac{r_2}{r_1})\Gamma\left(1+\frac{\xi_1^2}{r_1}\right)}{2(\xi_2^2-\xi_1^2\frac{r_2}{r_1})\Gamma(\alpha_1)\Gamma(\alpha_2)\Gamma(\beta_1)\Gamma(\beta_2)}\left(\frac{C\,(\alpha_1\beta_1 h_1)^{r_1}\,(\alpha_2\beta_2 h_2)^{r_2}}{s\mu_{r_1}\mu_{r_2}}\right)^{\frac{\xi_1^2}{r_1}}\\
&+\frac{\xi_1^2\xi_2^2\Gamma(\beta_1-\alpha_1)\Gamma(\alpha_2-\alpha_1\frac{r_2}{r_1})\Gamma(\beta_2-\alpha_1\frac{r_2}{r_1})\Gamma\left(1+\frac{\alpha_1}{r_1}\right)}{2(\xi_1^2-\alpha_1)(\xi_2^2-\alpha_1\frac{r_2}{r_1})\Gamma(1+\alpha_1)\Gamma(\alpha_2)\Gamma(\beta_1)\Gamma(\beta_2)}\left(\frac{C\,(\alpha_1\beta_1 h_1)^{r_1}\,(\alpha_2\beta_2 h_2)^{r_2}}{s\mu_{r_1}\mu_{r_2}}\right)^{\frac{\alpha_1}{r_1}}\\
&+\frac{\xi_1^2\xi_2^2\Gamma(\alpha_1-\beta_1)\Gamma(\alpha_2-\beta_1\frac{r_2}{r_1})\Gamma(\beta_2-\beta_1\frac{r_2}{r_1})\Gamma\left(1+\frac{\beta_1}{r_1}\right)}{2(\xi_1^2-\beta_1)(\xi_2^2-\beta_1\frac{r_2}{r_1})\Gamma(\alpha_1)\Gamma(\alpha_2)\Gamma(1+\beta_1)\Gamma(\beta_2)}\left(\frac{C\,(\alpha_1\beta_1 h_1)^{r_1}\,(\alpha_2\beta_2 h_2)^{r_2}}{s\mu_{r_1}\mu_{r_2}}\right)^{\frac{\beta_1}{r_1}}\\
&+\frac{\xi_1^2\Gamma(\alpha_1-\xi_2^2\frac{r_1}{r_2})\Gamma(\beta_1-\xi_2^2\frac{r_1}{r_2})\Gamma(\alpha_2-\xi_2^2)\Gamma(\beta_2-\xi_2^2)\Gamma\left(1+\frac{\xi_2^2}{r_2}\right)}{(\xi_1^2-\xi_2^2\frac{r_1}{r_2})\Gamma(\alpha_1)\Gamma(\alpha_2)\Gamma(\beta_1)\Gamma(\beta_2)}\left(\frac{C\,(\alpha_1\beta_1 h_1)^{r_1}\,(\alpha_2\beta_2 h_2)^{r_2}}{s\mu_{r_1}\mu_{r_2}}\right)^{\frac{\xi_2^2}{r_2}}\\
&+\frac{\xi_1^2\xi_2^2\Gamma(\alpha_1-\alpha_2\frac{r_1}{r_2})\Gamma(\beta_1-\alpha_2\frac{r_1}{r_2})\Gamma(\beta_2-\alpha_2)\Gamma\left(1+\frac{\alpha_2}{r_2}\right)}{(\xi_1^2-\alpha_2\frac{r_1}{r_2})(\xi_2^2-\alpha_2)\Gamma(\alpha_1)\Gamma(1+\alpha_2)\Gamma(\beta_1)\Gamma(\beta_2)}\left(\frac{C\,(\alpha_1\beta_1 h_1)^{r_1}\,(\alpha_2\beta_2 h_2)^{r_2}}{s\mu_{r_1}\mu_{r_2}}\right)^{\frac{\alpha_2}{r_2}}\\
&+\frac{\xi_1^2\xi_2^2\Gamma(\alpha_1-\beta_2\frac{r_1}{r_2})\Gamma(\beta_1-\beta_2\frac{r_1}{r_2})\Gamma(\alpha_2-\beta_2)\Gamma\left(1+\frac{\beta_2}{r_2}\right)}{(\xi_1^2-\beta_2\frac{r_1}{r_2})(\xi_2^2-\beta_2)\Gamma(\alpha_1)\Gamma(\alpha_2)\Gamma(\beta_1)\Gamma(1+\beta_2)}\left(\frac{C\,(\alpha_1\beta_1 h_1)^{r_1}\,(\alpha_2\beta_2 h_2)^{r_2}}{s\mu_{r_1}\mu_{r_2}}\right)^{\frac{\beta_2}{r_2}}.
\end{aligned} \tag{15}$$

This article has been accepted for publication in a future issue of this journal, but has not been fully edited. Content may change prior to final publication. Citation information: DOI 10.1109/TWC.2016.2630680, IEEE Transactions on Wireless Communications

D. Moments

The nth moments of the end-to-end SNR of a dual-hop FSO system using both types of detection techniques, defined as $\mathbb{E}[\gamma^n] = \int_0^\infty \gamma^n f_\gamma(\gamma)\, d\gamma$, can be shown to be given in terms of the Fox's H function by

$$\mathbb{E}[\gamma^n] = \frac{\xi_1^2\, \xi_2^2\, \Gamma(r_1 n + \alpha_1)\, \Gamma(r_1 n + \beta_1)\, \mu_{r_1}^n}{\Gamma(\alpha_1)\Gamma(\alpha_2)\Gamma(\beta_1)\Gamma(\beta_2)\Gamma(n)(r_1 n + \xi_1^2)(\alpha_1\beta_1 h_1)^{r_1 n}} \times \mathrm{H}_{2,4}^{4,1}\left[\frac{C\,(\alpha_2\beta_2 h_2)^{r_2}}{\mu_{r_2}} \middle| \begin{matrix}(1-n,1)(1+\xi_2^2, r_2) \\ (\xi_2^2, r_2)(\alpha_2, r_2)(\beta_2, r_2)(0,1)\end{matrix}\right]. \tag{16}$$

Proof: See Appendix D. ∎

Note that an efficient MATHEMATICA implementation for evaluating the Fox's H function $\mathrm{H}_{\cdot,\cdot}^{\cdot,\cdot}(\cdot)$ is presented in [47]. Furthermore, in the special case of a dual-hop FSO system operating under heterodyne detection (i.e. $r_1 = 1$ and $r_2 = 1$), (16) simplifies to

$$\mathbb{E}^H[\gamma^n] = \frac{\xi_1^2\, \xi_2^2\, \Gamma(n + \alpha_1)\, \Gamma(n + \beta_1)\, \mu_{r_1}^n}{\Gamma(\alpha_1)\Gamma(\alpha_2)\Gamma(\beta_1)\Gamma(\beta_2)\Gamma(n)(n + \xi_1^2)(\alpha_1\beta_1 h_1)^{n}} \times \mathrm{G}_{2,4}^{4,1}\left[\frac{C\alpha_2\beta_2 h_2}{\mu_{r_2}} \middle| \begin{matrix}1-n, 1+\xi_2^2 \\ \xi_2^2, \alpha_2, \beta_2, 0\end{matrix}\right]. \tag{17}$$

It is worthy to mention that the moments expressions in (16) and (17) are useful to obtain closed-form expressions for the n^{th}-order amount of fading given as [48]

$$AF_\gamma^{(n)} = \frac{\mathbb{E}[\gamma^n]}{\mathbb{E}[\gamma]^n} - 1. \tag{18}$$

IV. End-to-End Performance Metrics

A. Outage Probability

The outage probability is a standard performance metric of an FSO communication system. It is defined as the probability that the end-to-end SNR, γ, falls below a certain specified threshold, γ_{th}. An exact closed-form expression for the outage probability of dual-hop fixed gain relaying FSO systems in operation under both heterodyne detection as well as IM/DD with pointing error impairments can be easily obtained from (8), that is, $P_{\text{out}} = F_\gamma(\gamma_{\text{th}})$.

B. Average Bit-Error Rate

1) Exact Analysis: A unified expression for the average BER can be given in a compact form as

$$P_e = \frac{\delta}{2\Gamma(p)} \sum_{k=1}^{n} \int_0^\infty \Gamma(p, q_k\, \gamma) f_\gamma(\gamma)\, d\gamma, \tag{19}$$

where n, δ, p, and q_k vary depending on the type of detection (heterodyne technique or IM/DD) and modulation being assumed. It is worth accentuating that this expression is general enough to be used for both heterodyne and IM/DD techniques and can be applicable to different modulation schemes. Prior to presenting the unified BER closed-form results, we shall introduce Theorem 1 as follows

Theorem 1. *Let $a, b \in \mathbb{R}_+^*$. Define $I(a,b)$ as $I(a,b) = \frac{1}{2\Gamma(a)} \int_0^\infty \Gamma(a, b\,\gamma) f_\gamma(\gamma)\, d\gamma$, then $I(a,b)$ can be expressed in closed-form in terms of the bivariate Fox's H function as*

$$I(a,b) = \frac{1}{2} - \frac{\xi_1^2\, \xi_2^2}{2 r_1 r_2 \Gamma(\alpha_1)\Gamma(\alpha_2)\Gamma(\beta_1)\Gamma(\beta_2)\Gamma(a)} \mathrm{H}_{1,0:1,4:3,3}^{0,1:4,0:1,3} \left[\begin{matrix}(1, \frac{1}{r_2}, \frac{1}{r_1}) \\ - \\ (1+\xi_2^2, 1) \\ (\xi_2^2, 1)(\alpha_2, 1)(\beta_2, 1)(0, \frac{1}{r_2}) \\ (1-\xi_1^2, 1)(1-\alpha_1, 1)(1-\beta_1, 1) \\ (a, \frac{1}{r_1})(-\xi_1^2, 1)(0, \frac{1}{r_1})\end{matrix} \middle| \alpha_2\beta_2 h_2 \left(\frac{C}{\mu_{r_2}}\right)^{\frac{1}{r_2}}, \frac{(b\,\mu_{r_1})^{\frac{1}{r_1}}}{\alpha_1\beta_1 h_1}\right]. \tag{20}$$

Proof. See Appendix E. □

Based on Theorem 1, we get a general expression of the average BER for OOK, M-QAM, and M-PSK modulations as follows

$$P_e = \delta \sum_{k=1}^{n} I(p, q_k), \tag{21}$$

where n, δ, p, q_k are summarized in Table I.

2) High SNR Analysis: The average BER expression in (19) can be rewritten in terms of the CDF of γ by using integration by parts as

$$\overline{P}_e = \frac{\delta q_k^p}{2\Gamma(p)} \sum_{k=1}^{n} \int_0^\infty \gamma^{p-1} e^{-q_k\gamma} F_\gamma(\gamma)\, d\gamma. \tag{22}$$

Utilizing (22) together with (10), we obtain a very tight asymptotic expression of the average BER at high SNR in terms of simple elementary functions as shown in (23).

Table I: Parameters for Different Modulations [a]

Modulation Scheme	$\boldsymbol{\delta}$	$\boldsymbol{p}$	$\boldsymbol{q_k}$	$\boldsymbol{n}$	**Detection Type**
OOK	1	1/2	1/2	1	IM/DD
BPSK	1	1/2	1	1	Heterodyne
M-PSK	$\frac{2}{\max(\log_2 M, 2)}$	1/2	$\sin^2\left(\frac{(2k-1)\pi}{M}\right)$	$\max\left(\frac{M}{4}, 1\right)$	Heterodyne
M-QAM	$\frac{4}{\log_2 M}\left(1 - \frac{1}{\sqrt{M}}\right)$	1/2	$\frac{3(2k-1)^2}{2(M-1)}$	$\frac{\sqrt{M}}{2}$	Heterodyne

[a] In case of OOK modulation, the parameters δ, p , q_k , and n are determined via [46, Eq.(26)] and in case of M-PSK and M-QAM modulation schemes, these parameters may be determined utilizing [31, Eqs.(30) and (31)].

This article has been accepted for publication in a future issue of this journal, but has not been fully edited. Content may change prior to final publication. Citation information: DOI 10.1109/TWC.2016.2630680, IEEE Transactions on Wireless Communications

$$\overline{P_e}_{\mu_{r_1},\mu_{r_2}\gg 1}\approx \frac{\delta\Gamma(\alpha_1-\xi_1^2)\Gamma(\beta_1-\xi_1^2)\Gamma(\frac{\xi_1^2}{r_1}+p)}{2\Gamma(\alpha_1)\Gamma(\beta_1)\Gamma(p)}\sum_{k=1}^{n}\left(\frac{(\alpha_1\beta_1 h_1)^{r_1}}{q_k\,\mu_{r_1}}\right)^{\frac{\xi_1^2}{r_1}}$$
$$+\frac{\delta\xi_1^2\Gamma(\beta_1-\alpha_1)\Gamma(\frac{\alpha_1}{r_1}+p)}{2(\xi_1^2-\alpha_1)\Gamma(1+\alpha_1)\Gamma(\beta_1)\Gamma(p)}\sum_{k=1}^{n}\left(\frac{(\alpha_1\beta_1 h_1)^{r_1}}{q_k\,\mu_{r_1}}\right)^{\frac{\alpha_1}{r_1}}+\frac{\delta\xi_1^2\Gamma(\alpha_1-\beta_1)\Gamma(\frac{\beta_1}{r_1}+p)}{2(\xi_1^2-\beta_1)\Gamma(\alpha_1)\Gamma(1+\beta_1)\Gamma(p)}\sum_{k=1}^{n}\left(\frac{(\alpha_1\beta_1 h_1)^{r_1}}{q_k\,\mu_{r_1}}\right)^{\frac{\beta_1}{r_1}}$$
$$+\frac{\delta\xi_2^2\Gamma(\alpha_1-\xi_1^2)\Gamma(\beta_1-\xi_1^2)\Gamma(\alpha_2-\xi_1^2\frac{r_2}{r_1})\Gamma(\beta_2-\xi_1^2\frac{r_2}{r_1})\Gamma(\frac{\xi_1^2}{r_1}+p)}{4(\xi_2^2-\xi_1^2\frac{r_2}{r_1})\Gamma(\alpha_1)\Gamma(\alpha_2)\Gamma(\beta_1)\Gamma(\beta_2)\Gamma(p)}\sum_{k=1}^{n}\left(\frac{C\,(\alpha_1\beta_1 h_1)^{r_1}\,(\alpha_2\beta_2 h_2)^{r_2}}{q_k\,\mu_{r_1}\mu_{r_2}}\right)^{\frac{\xi_1^2}{r_1}}$$
$$+\frac{\delta\xi_1^2\xi_2^2\Gamma(\beta_1-\alpha_1)\Gamma(\alpha_2-\alpha_1\frac{r_2}{r_1})\Gamma(\beta_2-\alpha_1\frac{r_2}{r_1})\Gamma(\frac{\alpha_1}{r_1}+p)}{4(\xi_1^2-\alpha_1)(\xi_2^2-\alpha_1\frac{r_2}{r_1})\Gamma(1+\alpha_1)\Gamma(\alpha_2)\Gamma(\beta_1)\Gamma(\beta_2)\Gamma(p)}\sum_{k=1}^{n}\left(\frac{C\,(\alpha_1\beta_1 h_1)^{r_1}\,(\alpha_2\beta_2 h_2)^{r_2}}{q_k\,\mu_{r_1}\mu_{r_2}}\right)^{\frac{\alpha_1}{r_1}}$$
$$+\frac{\delta\xi_1^2\xi_2^2\Gamma(\alpha_1-\beta_1)\Gamma(\alpha_2-\beta_1\frac{r_2}{r_1})\Gamma(\beta_2-\beta_1\frac{r_2}{r_1})\Gamma(\frac{\beta_1}{r_1}+p)}{4(\xi_1^2-\beta_1)(\xi_2^2-\beta_1\frac{r_2}{r_1})\Gamma(\alpha_1)\Gamma(\alpha_2)\Gamma(1+\beta_1)\Gamma(\beta_2)\Gamma(p)}\sum_{k=1}^{n}\left(\frac{C\,(\alpha_1\beta_1 h_1)^{r_1}\,(\alpha_2\beta_2 h_2)^{r_2}}{q_k\,\mu_{r_1}\mu_{r_2}}\right)^{\frac{\beta_1}{r_1}}$$
$$+\frac{\delta\xi_1^2\Gamma(\alpha_1-\xi_2^2\frac{r_1}{r_2})\Gamma(\beta_1-\xi_2^2\frac{r_1}{r_2})\Gamma(\alpha_2-\xi_2^2)\Gamma(\beta_2-\xi_2^2)\Gamma(\frac{\xi_2^2}{r_2}+p)}{2(\xi_1^2-\xi_2^2\frac{r_1}{r_2})\Gamma(\alpha_1)\Gamma(\alpha_2)\Gamma(\beta_1)\Gamma(\beta_2)\Gamma(p)}\sum_{k=1}^{n}\left(\frac{C\,(\alpha_1\beta_1 h_1)^{r_1}\,(\alpha_2\beta_2 h_2)^{r_2}}{q_k\,\mu_{r_1}\mu_{r_2}}\right)^{\frac{\xi_2^2}{r_2}}$$
$$+\frac{\delta\xi_1^2\xi_2^2\Gamma(\alpha_1-\alpha_2\frac{r_1}{r_2})\Gamma(\beta_1-\alpha_2\frac{r_1}{r_2})\Gamma(\beta_2-\alpha_2)\Gamma(\frac{\alpha_2}{r_2}+p)}{2(\xi_1^2-\alpha_2\frac{r_1}{r_2})(\xi_2^2-\alpha_2)\Gamma(\alpha_1)\Gamma(1+\alpha_2)\Gamma(\beta_1)\Gamma(\beta_2)\Gamma(p)}\sum_{k=1}^{n}\left(\frac{C\,(\alpha_1\beta_1 h_1)^{r_1}\,(\alpha_2\beta_2 h_2)^{r_2}}{q_k\,\mu_{r_1}\mu_{r_2}}\right)^{\frac{\alpha_2}{r_2}}$$
$$+\frac{\delta\xi_1^2\xi_2^2\Gamma(\alpha_1-\beta_2\frac{r_1}{r_2})\Gamma(\beta_1-\beta_2\frac{r_1}{r_2})\Gamma(\alpha_2-\beta_2)\Gamma(\frac{\beta_2}{r_2}+p)}{2(\xi_1^2-\beta_2\frac{r_1}{r_2})(\xi_2^2-\beta_2)\Gamma(\alpha_1)\Gamma(\alpha_2)\Gamma(\beta_1)\Gamma(1+\beta_2)\Gamma(p)}\sum_{k=1}^{n}\left(\frac{C\,(\alpha_1\beta_1 h_1)^{r_1}\,(\alpha_2\beta_2 h_2)^{r_2}}{q_k\mu_{r_1}\mu_{r_2}}\right)^{\frac{\beta_2}{r_2}}. \tag{23}$$

Furthermore, the diversity order of the dual-hop FSO system can be given by

$$G_d=\min\left(\frac{\xi_1^2}{r_1},\frac{\alpha_1}{r_1},\frac{\beta_1}{r_1},\frac{\xi_2^2}{r_2},\frac{\alpha_2}{r_2},\frac{\beta_2}{r_2}\right). \tag{24}$$

C. Ergodic Capacity

The ergodic capacity of dual-hop FSO communication systems in operation under both heterodyne technique and IM/DD can be given by [49, Eq.(26)], [50, Eq.(7.43)], [51, Eq.(15)],

$$\overline{C}\triangleq\frac{1}{2}\,\mathbb{E}[\ln(1+c\,\gamma)]=\frac{1}{2}\int_0^\infty \ln(1+c\,\gamma)f_\gamma(\gamma)\,d\gamma, \tag{25}$$

where the factor $\frac{1}{2}$ is used because the relay terminal R is assumed to be operating in half-duplex mode, and c is a constant such that $c=e/(2\pi)$ for IM/DD technique (i.e. $r_i=2$) and $c=1$ for heterodyne technique (i.e. $r_i=1$) for $i\in(1,2)$. Note that the expression in (25) is exact for $r_i=1$ while it is a lower-bound for $r_i=2$, and can be derived in closed-form in terms of the bivariate Fox's H function as

$$\overline{C}=\frac{\xi_1^2\,\xi_2^2}{2\,r_1r_2\,\Gamma(\alpha_1)\Gamma(\alpha_2)\Gamma(\beta_1)\Gamma(\beta_2)}\mathrm{H}_{1,0:1,4:4,3}^{0,1:4,0:1,4}\left[\begin{array}{c|c|c}\begin{array}{c}(1,\frac{1}{r_2},\frac{1}{r_1})\\-\\(1+\xi_2^2,1)\\(\xi_2^2,1)(\alpha_2,1)(\beta_2,1)(0,\frac{1}{r_2})\\(1-\xi_1^2,1)(1-\alpha_1,1)(1-\beta_1,1)(1,\frac{1}{r_1})\\(1,\frac{1}{r_1})(-\xi_1^2,1)(0,\frac{1}{r_1})\end{array} & \alpha_2\beta_2 h_2\left(\frac{C}{\mu_{r_2}}\right)^{\frac{1}{r_2}},\frac{(c\,\mu_{r_1})^{\frac{1}{r_1}}}{\alpha_1\beta_1 h_1}\end{array}\right] \tag{26}$$

Proof: See Appendix F. ■

In the special case when the two FSO links use the heterodyne detection technique (i.e. $r_1=1$ and $r_2=1$), the ergodic capacity in (26) further simplifies to

$$\overline{C}^H=\frac{\xi_1^2\,\xi_2^2}{2\,r_1r_2\,\Gamma(\alpha_1)\Gamma(\alpha_2)\Gamma(\beta_1)\Gamma(\beta_2)}\mathrm{G}_{1,0:1,4:4,3}^{0,1:4,0:1,4}\left[\begin{array}{c|c|c}1 & 1+\xi_2^2 & 1-\xi_1^2,1-\alpha_1,1-\beta_1,1\\-&\xi_2^2,\alpha_2,\beta_2,0&1,-\xi_1^2,0\end{array}\left|\begin{array}{c}\frac{\alpha_2\beta_2 h_2 C}{\mu_{r_2}},\frac{c\,\mu_{r_1}}{\alpha_1\beta_1 h_1}\end{array}\right.\right]. \tag{27}$$

V. Numerical Results

In this section, we provide some numerical results to illustrate the mathematical formalism presented above and prove its correctness by means of Monte Carlo simulations. Without loss of generality, we assume equal average SNRs of both the links, $\overline{\gamma}_1=\overline{\gamma}_2=\overline{\gamma}$ with turbulence parameters for S-R and R-D FSO links $\alpha_1=\alpha_2=\alpha$ and $\beta_1=\beta_2=\beta$ and pointing errors $\xi_1=\xi_2=\xi$, except for Fig. 3 and Fig. 5. The wavelength is assumed to be $\lambda=1550$ nm. A fixed relay gain $C=1.1$ is considered. Moderate turbulence is characterized by $C_n^2=3\times10^{-14}\mathrm{m}^{\frac{-2}{3}}$, whereas strong turbulence is associated with $C_n^2=1\times10^{-13}\mathrm{m}^{\frac{-2}{3}}$ [3].

Fig. 1 demonstrates the impact of the pointing error on the outage probability of a dual-hop FSO link with $L_{S-R}=L_{R-D}=1000$ m under moderate turbulence with turbulence parameters $\alpha=5.42$ and $\beta=3.79$ calculated from (5) and (6), respectively. Results for a single 2000 m long FSO link with turbulence parameters obtained from (5) and (6) as $\alpha=4$ and $\beta=1.65$, are also included for comparison purposes (we divide the single link into two 1000 m long links). The exact closed-form expression for the outage probability of a

This article has been accepted for publication in a future issue of this journal, but has not been fully edited. Content may change prior to final publication. Citation information: DOI 10.1109/TWC.2016.2630680, IEEE Transactions on Wireless Communications

single FSO link under both heterodyne detection and IM/DD is given in [52, Eq.(5)]. Clearly, we observe from Fig. 1 that

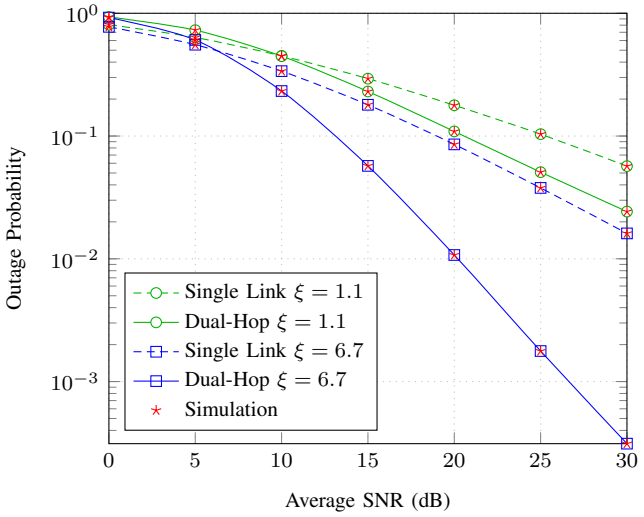

Fig. 1: Outage probability of single FSO and dual-hop FSO links for various values of ξ under moderate ($C_n^2 = 3 \times 10^{-14}\text{m}^{-\frac{2}{3}}$) turbulence conditions using IM/DD technique with a total length of 2000 m.

the analytical results provide a perfect match to the MATLAB simulated results proving the accuracy of our derivation. As expected, it can also be observed from this figure that for both dual-hop FSO and single FSO links, the outage probability performance degrades in the case of strong pointing errors. Furthermore, it can be seen that connecting two FSO links in series can significantly mitigate the pointing error impairments and as such improve the system performance, compared to the single FSO link. This result is in a perfect agreement with what was experimentally demonstrated in [33]. For example, at SNR=20 dB, for $\xi = 6.7$, the outage probability of the single FSO link is $P_{\text{out}} = 8.551300 \times 10^{-2}$ and it decreases to 1.07390010^{-2} in the case of the dual-hop FSO links.

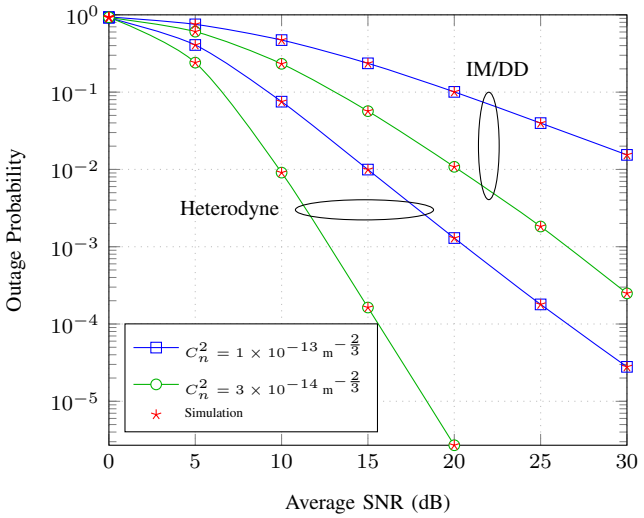

Fig. 2: Outage probability of a dual-hop FSO system for negligible pointing errors ($\xi_1 = \xi_2 = 6.7$) with strong ($C_n^2 = 1 \times 10^{-13}\text{m}^{-\frac{2}{3}}$) and moderate ($C_n^2 = 3 \times 10^{-14}\text{m}^{-\frac{2}{3}}$) turbulence conditions.

Fig. 2 depicts the outage probability performance of a dual-hop FSO system in the presence of moderate ($\alpha = 5.42$, $\beta = 3.79$) and strong ($\alpha = 4$, $\beta = 1.71$) turbulence conditions under both IM/DD and heterodyne detection for negligible effect of the pointing error ($\xi = 6.7$). We observe that for a given type of detection, P_{out} increases with an increase in the turbulence severity leading to a performance deterioration. It can also be shown that implementing heterodyne detection results in a considerable improvement in the dual-hop system performance compared to IM/DD, as expected. In fact, despite its complexity, heterodyne detection has been proposed as an alternative type of detection in FSO communication systems being able to better overcome the turbulence effects, relative to IM/DD technique [53]. For example, in the case of moderate turbulence, to achieve an outage probability of 10^{-3}, an SNR of 13 dB is required for the heterodyne detection technique while this increases to 26 dB when using the IM/DD technique.

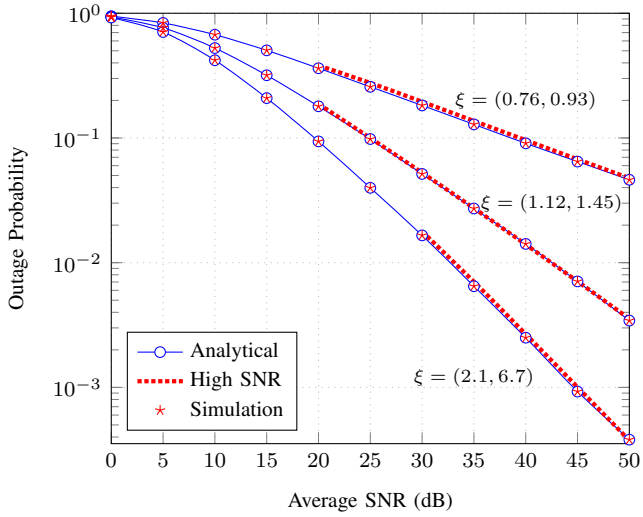

Fig. 3: Outage probability of a dual-hop FSO system using IM/DD technique for varying pointing errors along with the asymptotic results at high SNR.

The outage performance of the considered dual-hop system in operation under IM/DD technique (i.e. $r_1 = 2$ and $r_2 = 2$) for different pointing errors is illustrated in Fig. 3. The first FSO link undergoes strong turbulence and the second link undergoes moderate turbulence. It can be observed from Fig. 3 that the smaller the value of the pointing error parameter (i.e. the larger the value of the jitter), the stronger is the impact of the pointing error and therefore, the higher is the outage probability of the dual-hop FSO system. For example, at SNR=35 dB, the outage probability $P_{\text{out}} = 6.47 \times 10^{-3}$ for $\xi = (2.1, 6.7)$ and it increases to 2.72×10^{-2} and 1.29×10^{-1} when $\xi = (1.12, 1.45)$ and $\xi = (0.76, 0.93)$, respectively. The asymptotic results of the outage probability at high SNR values obtained by using (10) are also shown in Fig. 3. As clearly seen from this figure, the asymptotic results of the outage probability are in a perfect match with the analytical results in the high SNR regime. This observation justifies the accuracy and the tightness of the derived asymptotic expression in (10).

In Fig. 4, the average BER for 64-QAM, 16-QAM, 16-PSK,

This article has been accepted for publication in a future issue of this journal, but has not been fully edited. Content may change prior to final publication. Citation information: DOI 10.1109/TWC.2016.2630680, IEEE Transactions on Wireless Communications

and OOK modulation schemes of a dual-hop FSO system derived in (21) is plotted versus the average SNR, under strong turbulence conditions and negligible pointing errors. Moreover, this figure includes the average BER results for a single FSO link that experiences the Gamma-Gamma fading with pointing errors taken into account. Expectedly, it can be observed from Fig. 4 that the dual-hop FSO system offers better performance in terms of turbulence-induced fading mitigation for all types of modulation schemes, as compared with the single FSO link. This result, being experimentally verified in [33], emphasizes the effectiveness of the dual-hop FSO system in improving the performance of FSO links. For example, at BER=10^{-3}, using dual-hop relaying results in a SNR gain of approximately 10 dB for OOK, and 5 dB for 64-QAM, 16-QAM, and 16-PSK modulation schemes. Furthermore, it can be inferred from Fig. 4 that heterodyne systems using M-QAM or M-PSK modulations perform much better than IM/DD systems with OOK modulation. This performance enhancement is due the fact that heterodyne technique can better overcome the turbulence effects which comes at the expense of complexity in implementing coherent receivers relative to the IM/DD technique. It can also be noticed from Fig. 4 that 16-QAM outperforms 16-PSK, as expected.

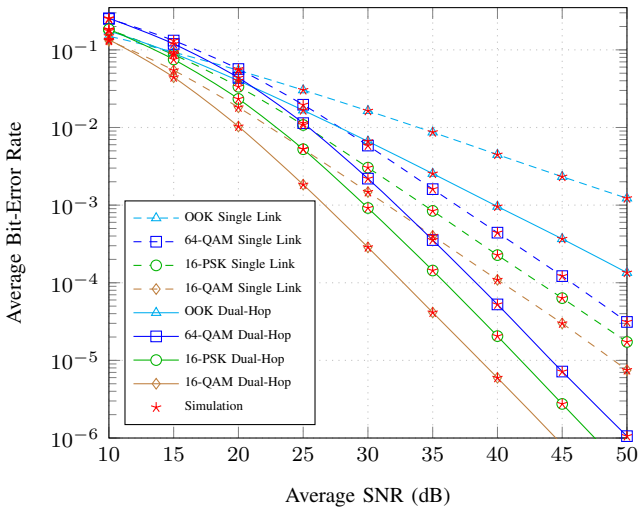

Fig. 4: Average BER for 64-QAM, 16-QAM, and 16-PSK and OOK modulation schemes of single FSO and dual-hop FSO links under strong turbulence conditions with negligible pointing errors for a total length of 2000 m.

Fig. 5 presents the average BER of dual-hop FSO IM/DD systems with OOK as well as dual-hop FSO heterodyne systems using different modulation schemes for strong pointing error $\xi = (1.12, 1.45)$. The first and the second FSO links are assumed to operate under strong and moderate turbulence conditions, respectively. It can be observed from Fig. 5 that the asymptotic expression of the average BER at high SNR given in (23) matches exactly the analytical expression derived in (21) proving the accuracy of the proposed asymptotic results at high SNR regime.

The ergodic capacity for both dual-hop FSO and single FSO links in operation under heterodyne detection as well as IM/DD is presented in Fig. 6. We can see from this figure that the analytical results of the ergodic capacity given by (26) for the dual-hop system and [52, Eq.(13)] for the single FSO link are in a good match with the simulated results. One of the most important outcomes of Fig. 6 is the capacity gain achieved by cascading two FSO links in series. For example, at SNR=30 dB, the capacity improves by 1.48% and 3.51% for IM/DD technique and heterodyne detection technique, respectively. Expectedly, it can be seen from this figure that heterodyne detection outperforms the IM/DD technique for both dual-hop and single FSO links.

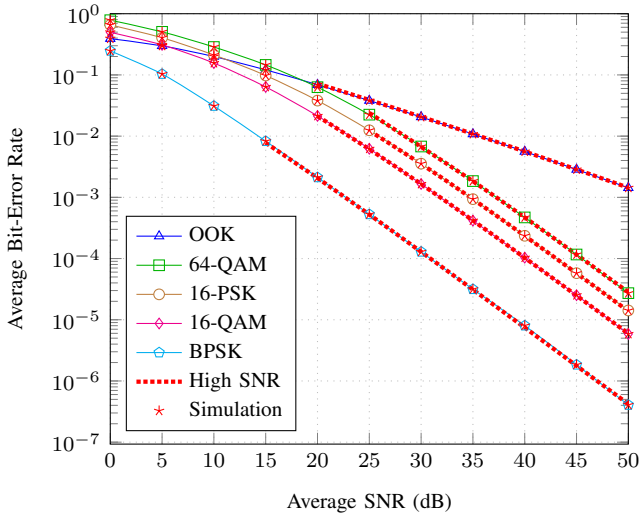

Fig. 5: Average BER for different modulation schemes of a dual-hop FSO system along with the asymptotic results at high SNR.

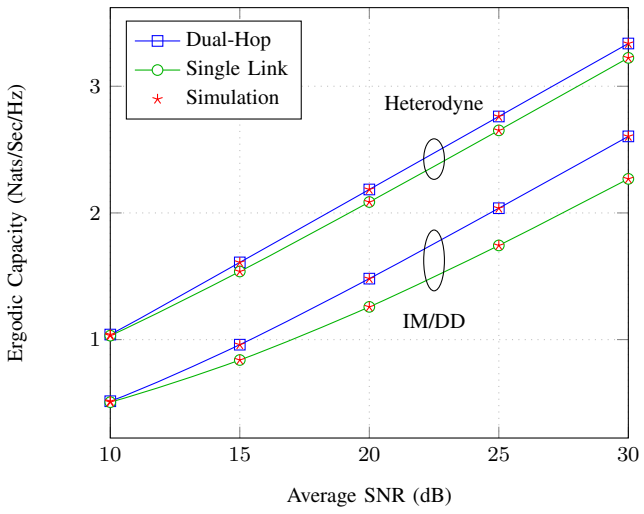

Fig. 6: Ergodic Capacity of single FSO and dual-hop FSO links under moderate turbulence conditions using both heterodyne detection and IM/DD with negligible pointing errors for a total propagation distance of 2000 m.

The ergodic capacity of the dual-hop FSO system in operation under IM/DD technique is presented in Fig. 7 for strong and moderate turbulence conditions with different pointing errors. It can be seen from this figure that as the effect of the turbulence and pointing error increases, the ergodic capacity degrades. Interestingly, it can observed that the effect of the turbulence conditions on the system capacity is more

This article has been accepted for publication in a future issue of this journal, but has not been fully edited. Content may change prior to final publication. Citation information: DOI 10.1109/TWC.2016.2630680, IEEE Transactions on Wireless Communications

intense when the FSO link undergoes negligible pointing errors ($\xi \to \infty$) as compared to the scenario when the FSO system is under severe pointing errors ($\xi \to 0$).

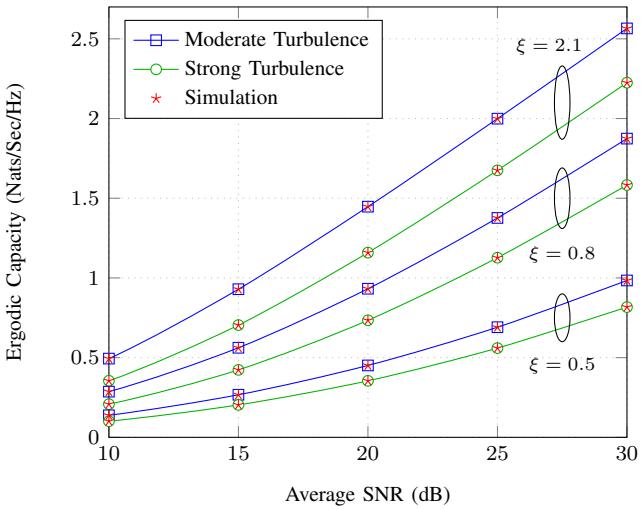

Fig. 7: Ergodic Capacity of a dual-hop FSO system using IM/DD technique under moderate and strong turbulence conditions for varying pointing errors.

VI. Conclusion

In this paper, we have investigated analytically for the first time the outage performance, the average BER, and the ergodic capacity of a dual-hop FSO system using AF fixed gain relaying in operation under both heterodyne detection as well as IM/DD including pointing error effects. In addition, tight asymptotic results for the outage probability and the average BER at high SNR have been derived in terms of simple functions. We demonstrated that the dual-hop FSO system outperforms the single FSO link and is capable of mitigating turbulence-induced fading and pointing errors. The effect of atmospheric turbulence and pointing errors on the dual-hop FSO link performance has also been studied and, as expected, severe pointing errors and strong turbulence can severely degrade the overall system performance of both single FSO and dual-hop FSO links.

Appendix A
CDF of the End-to-End SNR

In this appendix, we derive the CDF of the end-to-end SNR γ starting with

$$F_\gamma(\gamma) = \Pr\left[\frac{\gamma_1\,\gamma_2}{\gamma_2 + C} < \gamma\right], \tag{A.1}$$

which can be expressed as

$$\begin{aligned} F_\gamma(\gamma) &= \int_0^\infty \Pr\left[\frac{\gamma_1\,\gamma_2}{\gamma_2 + C} < \gamma | \gamma_2\right] f_{\gamma_2}(\gamma_2)\, d\gamma_2 \\ &= \int_0^\infty F_{\gamma_1}\left(\gamma\left(1 + \frac{C}{\gamma_2}\right)\right) f_{\gamma_2}(\gamma_2)\, d\gamma_2 \\ &= \int_{x=0}^\infty \int_{t=0}^{\gamma} f_{\gamma_1}(t) f_{\gamma_2}(x)\, dt\, dx \\ &\quad + \int_{x=0}^\infty \int_{t=\gamma}^{\gamma + \frac{C\gamma}{x}} f_{\gamma_1}(t) f_{\gamma_2}(x)\, dt\, dx. \end{aligned} \tag{A.2}$$

Integrating over the same area and interchanging the integrals yields

$$\begin{aligned} F_\gamma(\gamma) &= \int_{t=0}^{\gamma} \int_{x=0}^{\infty} f_{\gamma_2}(x) f_{\gamma_1}(t)\, dx\, dt \\ &\quad + \int_{t=\gamma}^{\infty} \int_{x=0}^{\frac{C\gamma}{t-\gamma}} f_{\gamma_2}(x) f_{\gamma_1}(t)\, dx\, dt \\ &= F_{\gamma_1}(\gamma) + \int_{\gamma}^{\infty} F_{\gamma_2}\left(\frac{C\gamma}{t-\gamma}\right) f_{\gamma_1}(t)\, dt. \end{aligned} \tag{A.3}$$

Substituting (2) and (7) in (A.3) we obtain

$$\begin{aligned} F_\gamma(\gamma) &= 1 - \frac{\xi_1^2\,\xi_2^2}{r_1\,\Gamma(\alpha_1)\Gamma(\alpha_2)\Gamma(\beta_1)\Gamma(\beta_2)} \\ &\times \int_\gamma^\infty \frac{1}{t} \mathrm{G}_{2,4}^{4,0}\left[\frac{\alpha_2\beta_2 h_2}{\mu_{r_2}^{\frac{1}{r_2}}}\left(\frac{C\gamma}{t-\gamma}\right)^{\frac{1}{r_2}} \middle| \begin{matrix} 1, \xi_2^2+1 \\ 0, \xi_2^2, \alpha_2, \beta_2 \end{matrix}\right] \\ &\times \mathrm{G}_{1,3}^{3,0}\left[\frac{\alpha_1\beta_1 h_1}{\mu_{r_1}^{\frac{1}{r_1}}} t^{\frac{1}{r_1}} \middle| \begin{matrix} \xi_1^2+1 \\ \xi_1^2, \alpha_1, \beta_1 \end{matrix}\right] dt. \end{aligned} \tag{A.4}$$

Using the change of variable $x = t - \gamma$ and the primary definition of the Meijer's G function in [44, Eq.(9.301)] with the integral identity [44, Eq.(3.194/3)], the CDF can be written as

$$\begin{aligned} F_\gamma(\gamma) &= 1 - \frac{\xi_1^2\,\xi_2^2}{r_1 r_2\,\Gamma(\alpha_1)\Gamma(\alpha_2)\Gamma(\beta_1)\Gamma(\beta_2)} \\ &\times \frac{1}{(2\pi i)^2} \int_{\mathcal{C}_1}\int_{\mathcal{C}_2} \Gamma\left(\frac{s}{r_2} + \frac{t}{r_1}\right) \\ &\times \frac{\Gamma(\xi_2^2 - s)\Gamma(\alpha_2 - s)\Gamma(\beta_2 - s)\Gamma(-\frac{s}{r_2})}{\Gamma(1 + \xi_2^2 - s)} \\ &\times \frac{\Gamma(\xi_1^2 + t)\Gamma(\alpha_1 + t)\Gamma(\beta_1 + t)}{\Gamma(\xi_1^2 + 1 + t)\Gamma(1 + \frac{t}{r_1})} \\ &\times \left(\alpha_2\beta_2 h_2\left(\frac{C}{\mu_{r_2}}\right)^{\frac{1}{r_2}}\right)^s \left(\frac{1}{\alpha_1\beta_1 h_1}\left(\frac{\mu_{r_1}}{\gamma}\right)^{\frac{1}{r_1}}\right)^t ds\, dt, \end{aligned} \tag{A.5}$$

where $\mathcal{C}_1$ and $\mathcal{C}_2$ are the s-plane and the t-plane contours, respectively. Now, by utilizing [41, Eq.(1.1)], we obtain the CDF expression of the end-to-end SNR given in (8).

Appendix B
High SNR Analysis

Using (A.5) and [41, Eq.(1.1)], the CDF can be written as

This article has been accepted for publication in a future issue of this journal, but has not been fully edited. Content may change prior to final publication. Citation information: DOI 10.1109/TWC.2016.2630680, IEEE Transactions on Wireless Communications

$$F_\gamma(\gamma) \approx 1 - \frac{\xi_1^2\xi_2^2}{2r_1r_2\Gamma(\alpha_1)\Gamma(\alpha_2)\Gamma(\beta_1)\Gamma(\beta_2)}\frac{1}{2\pi i}\int_{L_1} \times \frac{\Gamma(\xi_2^2-s)\Gamma(\alpha_2-s)\Gamma(\beta_2-s)\Gamma(-\frac{s}{r_2})}{\Gamma(1+\xi_2^2-s)}\left(\alpha_2\beta_2h_2\left(\frac{C}{\mu_{r_2}}\right)^{\frac{1}{r_2}}\right)^s \times \mathrm{H}_{2,4}^{4,0}\left[\alpha_1\beta_1h_1\left(\frac{\gamma}{\mu_{r_1}}\right)^{\frac{1}{r_1}}\middle|\begin{matrix}(1+\xi_1^2,1),(1,\frac{1}{r_1})\\(\frac{s}{r_2},\frac{1}{r_1}),(\xi_1^2,1),(\alpha_1,1),(\beta_1,1)\end{matrix}\right]ds - \frac{\xi_1^2\xi_2^2}{2r_1r_2\Gamma(\alpha_1)\Gamma(\alpha_2)\Gamma(\beta_1)\Gamma(\beta_2)}\frac{1}{2\pi i} \times \int_{L_2}\frac{\Gamma(\xi_1^2+t)\Gamma(\alpha_1+t)\Gamma(\beta_1+t)}{\Gamma(1+\xi_1^2+t)\Gamma(1+\frac{t}{r_1})}\left(\frac{\left(\frac{\mu_{r_1}}{\gamma}\right)^{\frac{1}{r_1}}}{\alpha_1\beta_1h_1}\right)^t \times \mathrm{H}_{2,4}^{4,1}\left[\alpha_2\beta_2h_2\left(\frac{C}{\mu_{r_2}}\right)^{\frac{1}{r_2}}\middle|\begin{matrix}(1-\frac{t}{r_1},\frac{1}{r_2}),(1+\xi_2^2,1)\\(\xi_2^2,1),(\alpha_2,1),(\beta_2,1),(0,\frac{1}{r_2})\end{matrix}\right]dt. \tag{B.1}$$

For high values of μ_{r_1} and μ_{r_2} the Fox's H functions in (B.1) can be approximated using the identity [40, Eq. (1.8.4)] as

$$\begin{aligned}&\mathrm{H}_{2,4}^{4,0}\left[\alpha_1\beta_1h_1\left(\frac{\gamma}{\mu_{r_1}}\right)^{\frac{1}{r_1}}\middle|\begin{matrix}(1+\xi_1^2,1),(1,\frac{1}{r_1})\\(\frac{s}{r_2},\frac{1}{r_1}),(\xi_1^2,1),(\alpha_1,1),(\beta_1,1)\end{matrix}\right]\\ &\underset{\mu_{r_1}\gg1}{\approx} r_1\frac{\Gamma(\xi_1^2-s\frac{r_1}{r_2})\Gamma(\alpha_1-s\frac{r_1}{r_2})\Gamma(\beta_1-s\frac{r_1}{r_2})}{\Gamma(1+\xi_1^2-s\frac{r_1}{r_2})\Gamma(1-\frac{s}{r_2})}\left((\alpha_1\beta_1h_1)^{r_1}\frac{\gamma}{\mu_{r_1}}\right)^{\frac{s}{r_2}}\\ &+\Gamma(\frac{s}{r_2}-\frac{\xi_1^2}{r_1})\frac{\Gamma(\alpha_1-\xi_1^2)\Gamma(\beta_1-\xi_1^2)}{\Gamma(1-\frac{\xi_1^2}{r_1})}\left((\alpha_1\beta_1h_1)^{r_1}\frac{\gamma}{\mu_{r_1}}\right)^{\frac{\xi_1^2}{r_1}}\\ &+\frac{\Gamma(\frac{s}{r_2}-\frac{\alpha_1}{r_1})\Gamma(\beta_1-\alpha_1)}{(\xi_1^2-\alpha_1)\Gamma(1-\frac{\alpha_1}{r_1})}\left((\alpha_1\beta_1h_1)^{r_1}\frac{\gamma}{\mu_{r_1}}\right)^{\frac{\alpha_1}{r_1}}\\ &+\frac{\Gamma(\frac{s}{r_2}-\frac{\beta_1}{r_1})\Gamma(\alpha_1-\beta_1)}{(\xi_1^2-\beta_1)\Gamma(1-\frac{\beta_1}{r_1})}\left((\alpha_1\beta_1h_1)^{r_1}\frac{\gamma}{\mu_{r_1}}\right)^{\frac{\beta_1}{r_1}},\end{aligned} \tag{B.2}$$

and

$$\begin{aligned}&\mathrm{H}_{2,4}^{4,1}\left[\alpha_2\beta_2h_2\left(\frac{C}{\mu_{r_2}}\right)^{\frac{1}{r_2}}\middle|\begin{matrix}(1-\frac{t}{r_1},\frac{1}{r_2}),(1+\xi_2^2,1)\\(\xi_2^2,1),(\alpha_2,1),(\beta_2,1),(0,\frac{1}{r_2})\end{matrix}\right]\\ &\underset{\mu_{r_2}\gg1}{\approx}\frac{r_2}{\xi_2^2}\Gamma(\alpha_2)\Gamma(\beta_2)\Gamma(\frac{t}{r_1})+\Gamma(\frac{t}{r_1}+\frac{\xi_2^2}{r_2})\Gamma(\alpha_2-\xi_2^2)\\ &\times\Gamma(\beta_2-\xi_2^2)\Gamma(-\frac{\xi_2^2}{r_2})\left((\alpha_2\beta_2h_2)^{r_2}\frac{C}{\mu_{r_2}}\right)^{\frac{\xi_2^2}{r_2}}\\ &+\Gamma(\frac{t}{r_1}+\frac{\alpha_2}{r_2})\frac{\Gamma(\beta_2-\alpha_2)\Gamma(-\frac{\alpha_2}{r_2})}{(\xi_2^2-\alpha_2)}\left((\alpha_2\beta_2h_2)^{r_2}\frac{C}{\mu_{r_2}}\right)^{\frac{\alpha_2}{r_2}}\\ &+\Gamma(\frac{t}{r_1}+\frac{\beta_2}{r_2})\frac{\Gamma(\alpha_2-\beta_2)\Gamma(-\frac{\beta_2}{r_2})}{(\xi_2^2-\beta_2)}\left((\alpha_2\beta_2h_2)^{r_2}\frac{C}{\mu_{r_2}}\right)^{\frac{\beta_2}{r_2}}\end{aligned} \tag{B.3}$$

Substituting (B.2) and (B.3) into (B.1) with some algebraic manipulations, we get the asymptotic expression of the CDF in the high SNR regime in (10).

Appendix C
PDF of the End-to-End SNR

Taking the derivative of (A.5) with respect to γ yields

$$\begin{aligned}f_\gamma(\gamma) = &-\frac{\xi_1^2\,\xi_2^2}{r_1r_2\,\Gamma(\alpha_1)\Gamma(\alpha_2)\Gamma(\beta_1)\Gamma(\beta_2)}\\ &\times\frac{1}{(2\pi i)^2}\int_{\mathcal{C}_1}\int_{\mathcal{C}_2}\Gamma\left(\frac{s}{r_2}+\frac{t}{r_1}\right)\\ &\times\frac{\Gamma(\xi_2^2-s)\Gamma(\alpha_2-s)\Gamma(\beta_2-s)\Gamma(-\frac{s}{r_2})}{\Gamma(1+\xi_2^2-s)}\\ &\times\frac{\Gamma(\xi_1^2+t)\Gamma(\alpha_1+t)\Gamma(\beta_1+t)}{\Gamma(\xi_1^2+1+t)\Gamma(1+\frac{t}{r_1})}\\ &\times\left(\alpha_2\beta_2h_2\left(\frac{C}{\mu_{r_2}}\right)^{\frac{1}{r_2}}\right)^s\left(\frac{\mu_{r_1}^{\frac{1}{r_1}}}{\alpha_1\beta_1h_1}\right)^t\frac{d\gamma^{-\frac{t}{r_1}}}{d\gamma}\,ds\,dt,\end{aligned} \tag{C.1}$$

which can be rewritten as

$$\begin{aligned}f_\gamma(\gamma) = &\frac{\xi_1^2\,\xi_2^2}{r_1r_2\,\Gamma(\alpha_1)\Gamma(\alpha_2)\Gamma(\beta_1)\Gamma(\beta_2)\gamma}\\ &\times\frac{1}{(2\pi i)^2}\int_{\mathcal{C}_1}\int_{\mathcal{C}_2}\Gamma\left(\frac{s}{r_2}+\frac{t}{r_1}\right)\\ &\times\frac{\Gamma(\xi_2^2-s)\Gamma(\alpha_2-s)\Gamma(\beta_2-s)\Gamma(-\frac{s}{r_2})}{\Gamma(1+\xi_2^2-s)}\\ &\times\frac{\frac{t}{r_1}\,\Gamma(\xi_1^2+t)\Gamma(\alpha_1+t)\Gamma(\beta_1+t)}{\Gamma(\xi_1^2+1+t)\Gamma(1+\frac{t}{r_1})}\\ &\times\left(\alpha_2\beta_2h_2\left(\frac{C}{\mu_{r_2}}\right)^{\frac{1}{r_2}}\right)^s\left(\frac{1}{\alpha_1\beta_1h_1}\left(\frac{\mu_{r_1}}{\gamma}\right)^{\frac{1}{r_1}}\right)^t ds\,dt.\end{aligned} \tag{C.2}$$

Using $\Gamma(1+\frac{t}{r_1}) = \frac{t}{r_1}\Gamma(\frac{t}{r_1})$, (C.2) can be further simplified yielding

$$\begin{aligned}f_\gamma(\gamma) = &\frac{\xi_1^2\,\xi_2^2}{r_1r_2\,\Gamma(\alpha_1)\Gamma(\alpha_2)\Gamma(\beta_1)\Gamma(\beta_2)\gamma}\\ &\times\frac{1}{(2\pi i)^2}\int_{\mathcal{C}_1}\int_{\mathcal{C}_2}\Gamma\left(\frac{s}{r_2}+\frac{t}{r_1}\right)\\ &\times\frac{\Gamma(\xi_2^2-s)\Gamma(\alpha_2-s)\Gamma(\beta_2-s)\Gamma(-\frac{s}{r_2})}{\Gamma(1+\xi_2^2-s)}\\ &\times\frac{\Gamma(\xi_1^2+t)\Gamma(\alpha_1+t)\Gamma(\beta_1+t)}{\Gamma(\xi_1^2+1+t)\Gamma(\frac{t}{r_1})}\\ &\times\left(\alpha_2\beta_2h_2\left(\frac{C}{\mu_{r_2}}\right)^{\frac{1}{r_2}}\right)^s\left(\frac{1}{\alpha_1\beta_1h_1}\left(\frac{\mu_{r_1}}{\gamma}\right)^{\frac{1}{r_1}}\right)^t ds\,dt.\end{aligned} \tag{C.3}$$

Applying [41, Eq.(1.1)], we get the desired PDF expression given by (11).

Appendix D
Moments

The moments can be written as

This article has been accepted for publication in a future issue of this journal, but has not been fully edited. Content may change prior to final publication. Citation information: DOI 10.1109/TWC.2016.2630680, IEEE Transactions on Wireless Communications

$$\mathbb{E}[\gamma^n] = \frac{\xi_1^2\,\xi_2^2}{r_1 r_2 \Gamma(\alpha_1)\Gamma(\alpha_2)\Gamma(\beta_1)\Gamma(\beta_2)} \int_0^\infty \frac{1}{x}\, \mathrm{H}_{0,1}^{1,0}\left[x \middle| \begin{matrix} - \\ (0,1) \end{matrix}\right] \times \mathrm{H}_{1,4}^{4,0}\left[\alpha_2\beta_2 h_2 \left(\frac{Cx}{\mu_{r_2}}\right)^{\frac{1}{r_2}} \middle| \begin{matrix} (1+\xi_2^2,1) \\ (\xi_2^2,1)(\alpha_2,1)(\beta_2,1)(0,\frac{1}{r_2}) \end{matrix}\right] \int_0^\infty \gamma^{n-1} \times \mathrm{H}_{3,2}^{0,3}\left[\frac{\left(\frac{\mu_{r_1}}{\gamma}x\right)^{\frac{1}{r_1}}}{\alpha_1\beta_1 h_1} \middle| \begin{matrix} (1-\xi_1^2,1)(1-\alpha_1,1)(1-\beta_1,1) \\ (-\xi_1^2,1)(1,\frac{1}{r_1}) \end{matrix}\right] d\gamma\, dx, \tag{D.1}$$

by means of substituting (11) into the definition of the moments then applying [41, Eq.(2.3)] to represent the the bivariate Fox's H function in terms of an integral involving the product of three Fox's H functions. Using [54, Eq.(1.59)] along with the Mellin transform of the Fox's H function given by [54, Eq.(2.8)], (D.1) reduces to

$$\mathbb{E}[\gamma^n] = \frac{\xi_1^2\,\xi_2^2\,\Gamma(r_1 n+\alpha_1)\,\Gamma(r_1 n+\beta_1)\,\mu_{r_1}^n}{\Gamma(\alpha_1)\Gamma(\alpha_2)\Gamma(\beta_1)\Gamma(\beta_2)\Gamma(n)(r_1 n+\xi_1^2)(\alpha_1\beta_1 h_1)^{r_1 n}} \times \int_0^\infty x^{n-1}\mathrm{H}_{0,1}^{1,0}\left[x \middle| \begin{matrix} - \\ (0,1) \end{matrix}\right] \times \mathrm{H}_{1,4}^{4,0}\left[\alpha_2\beta_2 h_2 \left(\frac{Cx}{\mu_{r_2}}\right)^{\frac{1}{r_2}} \middle| \begin{matrix} (1+\xi_2^2,1) \\ (\xi_2^2,1)(\alpha_2,1)(\beta_2,1)(0,\frac{1}{r_2}) \end{matrix}\right] dx. \tag{D.2}$$

Finally, employing [40, Eq.(2.8.4)] together with [54, Eq.(1.59)], the moments can easily simplify into (16) by means of some algebraic manipulations.

Appendix E
Average Bit-Error Rate

Substituting (A.5) into the definition of $I(a,b)$ and then utilizing [44, Eq.(3.381/4)], $I(a,b)$ may be written as

$$I(a,b) = \frac{1}{2} - \frac{\xi_1^2\,\xi_2^2}{2r_1 r_2\,\Gamma(\alpha_1)\Gamma(\alpha_2)\Gamma(\beta_1)\Gamma(\beta_2)} \frac{1}{(2\pi i)^2} \times \int_{\mathcal{C}_1}\int_{\mathcal{C}_2} \Gamma\left(\frac{s}{r_2}+\frac{t}{r_1}\right) \frac{\Gamma(\xi_2^2-s)\Gamma(\alpha_2-s)\Gamma(\beta_2-s)\Gamma(-\frac{s}{r_2})}{\Gamma(1+\xi_2^2-s)} \times \frac{\Gamma(\xi_1^2+t)\Gamma(\alpha_1+t)\Gamma(\beta_1+t)\Gamma(a-\frac{t}{r_1})}{\Gamma(\xi_1^2+1+t)\Gamma(1+\frac{t}{r_1})} \times \left(\alpha_2\beta_2 h_2\left(\frac{C}{\mu_{r_2}}\right)^{\frac{1}{r_2}}\right)^s \left(\frac{1}{\alpha_1\beta_1 h_1}\left(b\mu_{r_1}\right)^{\frac{1}{r_1}}\right)^t ds\, dt. \tag{E.1}$$

Using [41, Eq.(1.1)] results in the closed-form expression of $I(a,b)$ given in (20).

Appendix F
Ergodic Capacity

By substituting (C.3) into (25), the ergodic capacity can be written as

$$\overline{C} = \frac{\xi_1^2\,\xi_2^2}{2\,r_1 r_2\,\Gamma(\alpha_1)\Gamma(\alpha_2)\Gamma(\beta_1)\Gamma(\beta_2)} \frac{1}{(2\pi i)^2} \int_{\mathcal{C}_1}\int_{\mathcal{C}_2} \Gamma\left(\frac{s}{r_2}+\frac{t}{r_1}\right) \times \frac{\Gamma(\xi_2^2-s)\Gamma(\alpha_2-s)\Gamma(\beta_2-s)\Gamma(-\frac{s}{r_2})}{\Gamma(1+\xi_2^2-s)} \frac{\Gamma(\xi_1^2+t)\Gamma(\alpha_1+t)\Gamma(\beta_1+t)}{\Gamma(\xi_1^2+1+t)\Gamma(\frac{t}{r_1})} \times \left(\alpha_2\beta_2 h_2\left(\frac{C}{\mu_{r_2}}\right)^{\frac{1}{r_2}}\right)^s \left(\frac{\mu_{r_1}^{\frac{1}{r_1}}}{\alpha_1\beta_1 h_1}\right)^t \int_0^\infty \gamma^{-\frac{t}{r_1}-1}\,\ln(1+c\,\gamma)\, d\gamma\, ds\, dt. \tag{F.1}$$

Now, using [44, Eq.(4.293/10)] and [41, Eq.(1.1)], the ergodic capacity can be obtained in closed-form as in (26).

References

[1] L. C. Andrews, R. L. Phillips, and C. Y. Hopen, *Laser Beam Scintillation with Applications*. SPIE Press, 2001.

[2] K. Peppas and C. Datsikas, "Average symbol error probability of general-order rectangular quadrature amplitude modulation of optical wireless communication systems over atmospheric turbulence channels," *IEEE/OSA Journal of Optical Communications and Networking*, vol. 2, no. 2, pp. 102–110, Feb. 2010.

[3] W. Popoola and Z. Ghassemlooy, "BPSK subcarrier intensity modulated free-space optical communications in atmospheric turbulence," *IEEE/OSA Journal of Lightwave Technology*, vol. 27, no. 8, pp. 967–973, Apr. 2009.

[4] J. Park, E. Lee, and G. Yoon, "Average bit-error rate of the Alamouti scheme in Gamma-Gamma fading channels," *IEEE Photonics Technology Letters*, vol. 23, no. 4, pp. 269–271, 2011.

[5] M. Safari and M. Uysal, "Relay-assisted free-space optical communication," *IEEE Transactions on Wireless Communications*, vol. 7, no. 12, pp. 5441–5449, Dec. 2008.

[6] H. Sandalidis, T. Tsiftsis, G. Karagiannidis, and M. Uysal, "BER performance of FSO links over strong atmospheric turbulence channels with pointing errors," *IEEE Communications Letters*, vol. 12, no. 1, pp. 44–46, Jan. 2008.

[7] H. Sandalidis, T. Tsiftsis, and G. Karagiannidis, "Optical wireless communications with heterodyne detection over turbulence channels with pointing errors," *IEEE/OSA Journal of Lightwave Technology*, vol. 27, no. 20, pp. 4440–4445, Oct. 2009.

[8] W. Gappmair, "Further results on the capacity of free-space optical channels in turbulent atmosphere," *IET Communications*, vol. 5, no. 9, pp. 1262–1267, Jun. 2011.

[9] A. Al-Habash, L. Andrews, and R. Phillips, "Mathematical model for the irradiance probability density function of a laser beam propagating through turbulent media," *Optical Engineering*, vol. 40, no. 8, pp. 1554–1562, Aug. 2001.

[10] A. Farid and S. Hranilovic, "Outage capacity optimization for free-space optical links with pointing errors," *IEEE/OSA Journal of Lightwave Technology*, vol. 25, no. 7, pp. 1702–1710, Jul. 2007.

[11] M. Kuschnerov, F. N. Hauske, K. Piyawanno, B. Spinnler, M. S. Alfiad, A. Napoli, and B. Lankl, "DSP for coherent single-carrier receivers," *IEEE/OSA Journal of Lightwave Technology*, vol. 27, no. 16, pp. 3614–3622, Aug. 2009.

[12] M. G. Taylor, "Phase estimation methods for optical coherent detection using digital signal processing," *IEEE/OSA Journal of Lightwave Technology*, vol. 27, no. 7, pp. 901–914, Apr. 2009.

[13] R. Lange, B. Smutny, B. Wandernoth, R. Czichy, and D. Giggenbach, "142 km, 5.625 Gbps free-space optical link based on homodyne BPSK modulation," *Proceedings of SPIE, Free-Space Laser Communication Technologies XVIII*, vol. 6105, pp. 61 050A–61 050A–9, 2006.

[14] N. Cvijetic, D. Qian, J. Yu, Y. K. Huang, and T. Wang, "Polarization-multiplexed optical wireless transmission with coherent detection," *IEEE/OSA Journal of Lightwave Technology*, vol. 28, no. 8, pp. 1218–1227, Apr. 2010.

[15] D. L. Fried, "Optical heterodyne detection of an atmospherically distorted signal wave front," *Proceedings of the IEEE*, vol. 55, no. 1, pp. 57–77, Jan. 1967.

[16] J. H. Churnside and C. M. Mclntyre, "Heterodyne receivers for atmospheric optical communications," *Appl. Opt.*, vol. 19, no. 4, pp. 582–590, Feb. 1980.

[17] V. W. S. Chan, "Free-space optical communications," *IEEE/OSA Journal of Lightwave Technology*, vol. 24, no. 12, pp. 4750–4762, Dec. 2006.

[18] A. Acampora and S. Krishnamurthy, "A broadband wireless access network based on mesh-connected free-space optical links," *IEEE Personal Communications*, vol. 6, no. 5, pp. 62–65, Oct. 1999.

[19] G. Karagiannidis, T. Tsiftsis, and H. Sandalidis, "Outage probability of relayed free space optical communication systems," *Electronics Letters*, vol. 42, no. 17, pp. 994–995, Aug. 2006.

[20] M. Safari and M. Uysal, "Relay-assisted free-space optical communication," *IEEE Transactions on Wireless Communications*, vol. 7, no. 12, pp. 5441–5449, Dec. 2008.

[21] C. Datsikas, K. Peppas, N. Sagias, and G. Tombras, "Serial free-space optical relaying communications over Gamma-Gamma atmospheric turbulence channels," *IEEE/OSA Journal of Optical Communications and Networking*, vol. 2, no. 8, pp. 576–586, Aug. 2010.

[22] E. Lee, J. Park, D. Han, and G. Yoon, "Performance analysis of the asymmetric dual-hop relay transmission with mixed RF/FSO links," *IEEE Photonics Technology Letters*, vol. 23, no. 21, pp. 1642–1644, Nov. 2011.

[23] I. S. Ansari, F. Yilmaz, and M.-S. Alouini, "Impact of pointing errors on the performance of mixed RF/FSO dual-hop transmission systems," *IEEE Wireless Communications Letters*, vol. 2, no. 3, pp. 351–354, June 2013.

[24] H. Samimi and M. Uysal, "End-to-end performance of mixed RF/FSO transmission systems," *IEEE/OSA Journal of Optical Communications and Networking*, vol. 5, no. 11, pp. 1139–1144, Nov. 2013.

[25] I. S. Ansari, F. Yilmaz, and M.-S. Alouini, "On the performance of mixed RF/FSO variable gain dual-hop transmission systems with pointing errors," in *Proceedings of IEEE 78th Vehicular Technology Conference (VTC Fall' 2013)*, Las Vegas, USA, Sep. 2013, pp. 1–6.

[26] ——, "On the performance of hybrid RF and RF/FSO dual-hop transmission systems," in *2nd International Workshop on Optical Wireless Communications (IWOW' 2013)*, Newcastle, UK, Oct. 2013, pp. 45–49.

[27] N. Miridakis, M. Matthaiou, and G. Karagiannidis, "Multiuser relaying over mixed RF/FSO links," *IEEE Transactions on Communications*, vol. 62, no. 5, pp. 1634–1645, May 2014.

[28] E. Soleimani-Nasab and M. Uysal, "Generalized performance analysis of mixed RF/FSO systems," in *3rd International Workshop on Optical Wireless Communications (IWOW' 2014)*, Funchal, Portugal, Sep. 2014, pp. 16–20.

[29] E. Zedini, I. S. Ansari, and M.-S. Alouini, "Performance analysis of mixed Nakagami-m and Gamma-Gamma dual-hop FSO transmission systems," *IEEE Photonics Journal*, vol. 7, no. 1, pp. 1–20, Feb. 2015.

[30] E. Soleimani-Nasab and M. Uysal, "Generalized performance analysis of mixed RF/FSO cooperative systems," *IEEE Transactions on Wireless Communications*, vol. 15, no. 1, pp. 714–727, Jan. 2016.

[31] E. Zedini, H. Soury, and M. S. Alouini, "On the performance analysis of dual-hop mixed FSO/RF systems," *IEEE Transactions on Wireless Communications*, vol. 15, no. 5, pp. 3679–3689, May 2016.

[32] M. Aggarwal, P. Garg, and P. Puri, "Dual-hop optical wireless relaying over turbulence channels with pointing error impairments," *IEEE/OSA Journal of Lightwave Technology*, vol. 32, no. 9, May 2014.

[33] J. Libich, M. Komanec, S. Zvanovec, P. Pesek, W. Popoola, and Z. Ghassemlooy, "Experimental verification of an all-optical dual-hop 10 Gbit/s free-space optics link under turbulence regimes," *Optics Letters*, vol. 40, no. 3, pp. 391–394, Feb. 2015.

[34] X. Zhu and J. M. Kahn, "Free-space optical communication through atmospheric turbulence channels," *IEEE Transactions on Communications*, vol. 50, no. 8, pp. 1293–1300, Aug. 2002.

[35] S. B. E. A. and T. M. C., *Fundamentals of Photonics*. John Wiley & Sons, 1991.

[36] M. L. B. Riediger, R. Schober, and L. Lampe, "Fast multiple-symbol detection for free-space optical communications," *IEEE Transactions on Communications*, vol. 57, no. 4, pp. 1119–1128, Apr. 2009.

[37] M. Uysal, J. Li, and M. Yu, "Error rate performance analysis of coded Free-Space Sptical links over Gamma-Gamma atmospheric turbulence channels," *IEEE Transactions on Wireless Communications*, vol. 5, no. 6, pp. 1229–1233, Jun. 2006.

[38] M. Hasna and M.-S. Alouini, "A performance study of dual-hop transmissions with fixed gain relays," *IEEE Transactions on Wireless Communications*, vol. 3, no. 6, pp. 1963–1968, Nov. 2004.

[39] A. Prudnikov, Y. Brychkov, and O. Marichev, *Integrals and Series, Volume 3: More Special Functions*. CRC, 1999.

[40] A. Kilbas and M. Saigo, *H-Transforms : Theory and Applications (Analytical Method and Special Function)*, 1st ed. CRC Press, 2004.

[41] P. Mittal and K. Gupta, "An integral involving generalized function of two variables," *Proceedings of the Indian Academy of Sciences - Section A*, vol. 75, no. 3, pp. 117–123, 1972.

[42] K. Peppas, "A new formula for the average bit error probability of dual-hop amplify-and-forward relaying systems over generalized shadowed fading channels," *IEEE Wireless Communications Letters*, vol. 1, no. 2, pp. 85–88, Apr. 2012.

[43] I. S. Ansari, S. Al-Ahmadi, F. Yilmaz, M.-S. Alouini, and H. Yanikomeroglu, "A new formula for the BER of binary modulations with dual-branch selection over generalized-K composite fading channels," *IEEE Transactions on Communications*, vol. 59, no. 10, Oct. 2011.

[44] I. S. Gradshteyn and I. M. Ryzhik, *Table of Integrals, Series and Products*. New York: Academic Press, 2000.

[45] M. Simon and M.-S. Alouini, *Digital Communication over Fading Channels*, ser. Wiley series in telecommunications and signal processing. New York: Wiley, 2005.

[46] E. Zedini and M. S. Alouini, "Multihop relaying over IM/DD FSO systems with pointing errors," *IEEE/OSA Journal of Lightwave Technology*, vol. 33, no. 23, pp. 5007–5015, Dec. 2015.

[47] F. Yilmaz and M.-S. Alouini, "Product of the powers of generalized Nakagami-m variates and performance of cascaded fading channels," in *IEEE Global Telecommunications Conference (GLOBECOM'09)*, Nov. 2009, pp. 1–8.

[48] ——, "Novel asymptotic results on the high-order statistics of the channel capacity over generalized fading channels," in *IEEE 13th International Workshop on Signal Processing Advances in Wireless Communications (SPAWC'2012)*, 2012, pp. 389–393.

[49] A. Lapidoth, S. M. Moser, and M. A. Wigger, "On the capacity of free-space optical intensity channels," *IEEE Transactions on Information Theory*, vol. 55, no. 10, pp. 4449–4461, Oct. 2009.

[50] S. Arnon, J. Barry, G. Karagiannidis, R. Scober, and M. Uysal, *Advanced Optical Wireless Communications Systems*. Cambridge University Press, 2013.

[51] K. P. Peppas, A. N. Stassinakis, H. E. Nistazakis, and G. S. Tombras, "Capacity analysis of dual amplify-and-forward relayed free-space optical communication systems over turbulence channels with pointing errors," *IEEE/OSA Journal of Optical Communications and Networking*, vol. 5, no. 9, pp. 1032–1042, Sep. 2013.

[52] I. Ansari, F. Yilmaz, and M.-S. Alouini, "Performance analysis of FSO links over unified Gamma-Gamma turbulence channels," in *IEEE 81st Vehicular Technology Conference (VTC Spring' 2015)*, May 2015.

[53] T. Tsiftsis, "Performance of heterodyne wireless optical communication systems over Gamma-Gamma atmospheric turbulence channels," *Electronics Letters*, vol. 44, no. 5, pp. 372–373, Feb. 2008.

[54] A. Mathai, R. K. Saxena, and H. J. Haubold, *The H-Function: Theory and Applications*. Springer, 2010.